

Self-Assembly of Amphiphilic Discotic Materials

by
Welmarie van Schalkwyk

*Dissertation presented for the degree of Master of
Science in the Faculty of Science at
Stellenbosch University*



Supervisor: Prof Bert Klumperman

March 2013

Declaration

By submitting this thesis/dissertation electronically, I declare that the entirety of the work contained therein is my own, original work, that I am the sole author thereof (save to the extent explicitly otherwise stated), that reproduction and publication thereof by Stellenbosch University will not infringe any third party rights and that I have not previously in its entirety or in part submitted it for obtaining any qualification.

Welmarie van Schalkwyk

Date: March 2013

Abstract

The creation of nanometer-scale (nanoscale) materials has fascinated and inspired the scientific community for more than a quarter of a century because of the wide range of applications of these materials, e.g. applications in drug delivery, medicine, tissue engineering, memory storage, display and audio devices, semiconductors, etc.

π -Conjugated dendrimers have a proposed flat packing arrangement. An alternating phenyl isoxazole dendrimer system was developed to investigate this phenomenon. The synthesis of this dendritic system was attempted by divergent and convergent approaches. Preparation of the second generation failed because some functional groups inhibited the monomers to react to the first generation.

Other examples of nano materials that have attracted a vast amount of interest are the so-called discotic amphiphiles. Discotic amphiphilic molecules have the potential to self-assemble into helical architectures.

Discotic systems bearing chiral polar side chains (one and three respectively) were developed. Their self-assembly was investigated in variable concentration and variable solvent composition experiments. These systems did show signs of aggregation in UV-vis and CD spectroscopy experiments. Thread-like helical structures were observed with transmission electron microscopy.

Opsomming

Nanometer-skaal materiale inspireer en fassineer wetenskaplikes al vir meer as 25 jaar as gevolg van hulle wye verskeidenheid toepassings bv.: die vervoer van geneesmiddels, weefsel ontwerp, geheue stoorspasie, digitale skerms, klank toerusting, geleiers, ens.

π -Gekonjugeerde dendrimere het 'n plat drie dimmensionele rangskikking. 'n Afwisselende feniel isoxazole dendrimer stelsel was ontwikkel om hierdie verskynsel te ondersoek. Die sintese van hierdie dendritiese stelsel is aangepak deur divergerende en konvergerende benaderings. Sintese van die tweede generasie het misluk omdat sommige funksionele groepe die monomere geïnhibeer het om te reageer met die eerste generasie.

Ander interessante voorbeelde van nano materiale, is die sogenaamde skyfvormige amphiphiles. Skyfvormige amphiphiles het die potensiaal om spontaan te versamel in heliese strukture.

Skyfvormige molekules met chirale polêre sykettings (een en drie onderskeidelik) is ontwikkel. Hulle potensiaal om spontaan te versamel is ondersoek met wisselende konsentrasie en wisselende oplosmiddel samestelling eksperimente. Hierdie stelsels het tekens van versameling gewys in UV-vis en CD-spektroskopiese eksperimente. Staafvormige heliese strukture is waargeneem met transmissie-elektronmikroskopie.

Acknowledgements

I thank my promoter prof. Bert Klumperman for his guidance, advice, and the opportunity to pursue research under his supervision.

My special thanks are extended to Rueben Pfukwa for all his patience and guidance with this project. I really appreciate everything you have done for me.

I would also like to thank past and present members of the Klumperman research group: Njabu, Rueben, Waled, Paul, William, Ingrid, Erika, Nathalie, Lizl, Sandile, Siyasanga, Freda, Osama, Ahmed, Mpho, Lehani, Nicole, Ahson, Khotso, and Hamilton. Thank you for all the help, advice, and assistance.

I also thank prof. Willem van Otterlo for the valuable advice towards my synthetic work. Abu Taher (from the Van Otterlo Group) is thanked for synthetic work.

The Staff members at Polymer Science are thanked for all their help and assistance: Calvin Maart, Erinda Cooper, Deon Koen, Jim Motshweni, and Aneli Fourie.

I would like to thank everyone who helped with analysis work. Elsa Malherbe and Jaco Brand are kindly thanked for all their help with NMR and CD-experiments. Marietjie Stander and Hiten Fletcher are thanked for Mass Spec analysis.

The NRF and Stellenbosch University is thanked for funding this project.

I would also like to acknowledge my friends and family for their support. Life would be so boring without you.

Last but not least I would like to thank my parents for their love and support. I don't think there is anything I can say to acknowledge what you have done for me. I really appreciate everything you have given me in life.

Contents

Declaration	ii
Abstract.....	iii
Opsomming	iv
Acknowledgements.....	v
List of Figures.....	viii
List of Schemes	x
List of Abbreviations.....	xi
Chapter 1 Preface	1
1.1 Introduction	1
1.2 <i>Aim</i>	1
1.3 <i>Structure of the thesis</i>	1
1.4 <i>References</i>	3
Chapter 2 Self-Assembly and Packing of π -Conjugated Amphiphilic Materials	4
2.1 Helical Self-Assembly	6
Helical Self-Assembly of Conjugated Discotic Amphiphiles	9
2.1.1 π - π Stacking	10
2.1.2 Chiral Amplification of Discotic Molecules.....	13
2.1.3 Solvent effects	15
2.2 Characterization of Self-assembled Helical Aggregates.....	17
2.2.1 NMR-Spectroscopy.....	17
2.2.2 UV-Spectroscopy.....	17
2.2.3 Microscopy	17
2.2.4 Circular Dicroism	19
2.3 Approach.....	20
2.4 References:	21
Chapter 3 Synthesis of π -Conjugated Isoxazole Dendrimer Systems	24
3.1 Introduction.....	24
Dendrimer synthesis.....	25
3.2 Our approach	27
3.2.1 Divergent pathway.....	27
3.2.2 Convergent pathway.....	28
3.3 Results and discussion	28

3.3.1	Divergent Pathway	29
3.3.2	Convergent Pathway.....	34
3.4	Conclusions	35
3.5	Materials and Methods	35
3.5.1	Materials	35
3.5.2	Experimental Procedures.....	35
3.5	References.....	41
Chapter 4 Triazole Amphiphilic Materials.....		43
4.1	Introduction	43
4.2	Results and discussion	44
4.2.1	Mono side chain amphiphile	44
4.2.2	Tri side chain amphiphile	48
4.3	Conclusions	52
4.4	Materials an Methods.....	53
4.4.1	Materials	53
4.4.2	Experimental Procedures.....	53
4.5	References.....	58
Chapter 5 Conclusions		60
	Future work.....	60
References		62

List of Figures

- Figure 2.1. (a) The structure of the tobacco mosaic virus, (b)-(e) Self-assembly of the tobacco mosaic virus. 6
- Figure 2.2. Helical motifs in Nature: (a) the DNA double helix, (b) open and closed gramicidin A channels and (c) the triple helix of collagen. 7
- Figure 2.3. Examples of reported helical motifs; (a) Helical growth of chiral perylene bisimides, (b) Benzene-1,3,5-tricarboxamide core directs self-assembly into a helical architectures, (c) Self-assembly of OPV derivatives, (d) Self-assembly of discotic triamides, (e) Self-assembly of bipyridine-based molecules forming left- and right-handed helices, (f) Self-assembly of twisted stacks of N,N',N''-tris[3(3'-carbamoylamino)-2,2'-bipyridyl]-benzene-1,3,5-tricarbonamide derivatives. 8
- Figure 2.4. Examples of systems which form π - π stacking interactions in self-assembly: (a) Phenyl acetylene macrocycles, (b) Tetrathiafulvalene macrocycles, (c) Hexa-perihexabenzocoronenes' chemical structure and a schematic of their self-assembly into columns and aggregates, (d) Schematic representation of proposed self-assembly for formation of hexameric macrocycles. 12
- Figure 2.5. (a) Structure of discotic moieties, bearing either achiral or chiral side chains, for helical self-assembly, (b) Structures of discotic tris-amides and schematic representation of the supramolecular polymerisation process into helical stacks. 15
- Figure 2.6. (a),(b) TEM images of helical ribbon nano structures from rod-coil block copolymers, (c),(d) FESEM images of the xerogel of tris(phenylisoxazolyl)benzene derivative, (e)-(f) shows AFM images of an oligo(p-phenylenevinylene) derivate: (e) homoassembly, (f) coassembly of the initial achiral derivative with 9% chiral derivative, (g) coassembly of initial achiral derivative with 60% chiral derivative. 18
- Figure 2.7. (a) Variable temperature CD spectra in hexane, (b) Mirror image Cotton-effects observed for M- and P-Helices. 20
- Figure 3.1. Spartan representation of the second generation of a phenyl-isoxazole dendrimer: a) front view showing a supposed flat structure, b) side view showing fan-like out of plane structures. 25
- Figure 3.2. i) ^1H NMR spectrum of **12a** and ii) ^1H NMR spectrum of **12b** in chloroform- d_6 between 8.0-6.7ppm. 32
- Figure 3.3. ^1H NMR spectrum of 3,5-di-5-phenylisoxazole bromobenzene (**13**) in CDCl_3 . 33

- Figure 4.1. UV-vis spectra of **24**: (a) solvent dependent experiments varying the solvent from 100:0 DMF/ H₂O to 10:80 DMF/ H₂O (violet = lowest H₂O%, red = high H₂O%, (b) concentration dependent studies carried out in a 90:10 DMF/ H₂O solution. (red = lowest concentration 0.00272 mM; violet = highest concentration 0.272 mM). 46
- Figure 4.2. CD spectra of **24** (a) 100:0 acetonitrile/ H₂O to 10:90 acetonitrile/ H₂O (red line = 10:90 acetonitrile/ H₂O; orange line = 20:80 acetonitrile/ H₂O; other colours = 40:60 acetonitrile/ H₂O to 100:0 acetonitrile/ H₂O), (b) 10-90% H₂O solution in a mother solution of 10:90 DMF/ acetonitrile (red line = 90% H₂O; orange line = 80% H₂O and the rest of the colours is from 70-10% H₂O). 47
- Figure 4.3. ¹H NMR spectrum of **30** in DMSO-d₆. 50
- Figure 4.4. UV-vis spectra of **30** (a) Solvent dependent studies (red line = 10:90 H₂O/ DMF, lilac line = 100:0 H₂O/ DMF), (b) Absorbance at 279 nm plotted against the H₂O content. 51
- Figure 4.5. CD spectra of solvent dependent studies of **30** (red line = 100:0 H₂O/ DMF, lilac line = 10:90 H₂O/ DMF). 52
- Figure 4.6. TEM images of **30** in H₂O. 52

List of Schemes

Scheme 2.1. Schematic representation of the top-down (left to right) and bottom-up approaches (right to left) towards nanostructures.	4
Scheme 2.2 Folding of a random coil into a helical foldamer.	7
Scheme 2.3. Schematic of potential self-assembly arytriazole amphiphiles with chiral side chains (purple triangle represents the π -conjugated core).	10
Scheme 2.4. Self-assembly of tris(phenylisoxazolyl)benzene into helical structures showing the equilibrium between left- and right handed helices.	13
Scheme 2.5. Schematic representation of the sergeants-and-soldiers principle. In the first scheme both M- and P-Helices are obtained because of achiral side chains, while the second scheme forms a single handed helix because of the addition of a chiral molecule (orange side chains).	14
Scheme 3.1. Schematic representation of divergent and convergent approaches towards dendritic materials.	26
Scheme 3.2. Schematic representation of imidoyl chloride and oxime routes followed.	26
Scheme 3.3 Proposed synthesis route for divergent growth of isoxazole dendrimer.	27
Scheme 3.4. Illustration of convergent growth of isoxazole dendrimer.	28
Scheme 3.5. Synthesis of the dendrimer core.	30
Scheme 3.6 Synthesis of the dendrimer periphery.	30
Scheme 3.7. Attempted synthesis of the first generation via the imidoyl chloride route.	31
Scheme 3.8. Model study of isoxazole synthesis.	31
Scheme 3.9. Di-isoxazole synthesis in model study.	33
Scheme 3.10. Attempted synthesis of the second generation via the oxime pathway.	34
Scheme 3.11. Synthesis of 'new' periphery of isoxazole dendrimer via the convergent pathway.	34
Scheme 4.1. Proposed self-assembly of di-triazole amphiphile.	43
Scheme 4.2. Synthesis of chiral side chain.	45
Scheme 4.3. Synthesis of amphiphile bearing one side chain.	45
Scheme 4.4. Synthesis of terminal alkyne unit bearing chiral side chain.	49
Scheme 4.5. Synthesis of 30 .	49

List of Abbreviations

AFM	atomic force microscopy
CD	circular dichroism
CDCl ₃	deuterated chloroform
DCC	<i>N,N'</i> -dicyclohexylcarbodiimide
DCM	dichloromethane
DLC	discotic liquid crystals
DLS	dynamic light scattering
DMAP	4-dimethylaminopyridine
DMF	dimethylformamide
DMSO	dimethyl sulfoxide
DMSO-d ₆	deuterated dimethyl sulfoxide
DPA	dendritic polyphenylazomethine
FESEM	field-emission scanning electron microscopy
HBC	hexa-peri-hexabenzocoronenes
LiAlH ₄	lithium aluminium hydride
NBS	<i>N</i> -bromosuccinimide
NCS	<i>N</i> -chlorosuccinimide
NMR	nuclear magnetic resonance
OPE	oligo(phenylene ethynylene)
OPV	oligo(p-phenylenevinylene)
PBI	perylene bisimide
PCC	pyridinium chlorochromate
PEG	polyethylene glycol
PMDETA	<i>N,N,N',N',N''</i> -pentamethyldiethylenetriamine
SEM	scanning electron microscope
STM	scanning tunneling microscopy

TBAF	tetra- <i>n</i> -butylammonium fluoride
TEA	triethylamine
TEM	transmission electron microscopy
TFA	trifluoroacetic acid
THF	tetrahydrofuran
TLC	thin layer chromatography
TMV	tobacco mosaic virus
TPA	two-photon absorption
UV	ultra violet
VPO	vapor pressure osmometry

Chapter 1 Preface

1.1 Introduction

The helix is an interesting motif that is one of the most frequently occurring secondary structural motifs used in nature.¹ Synthesis of artificial helical structures with a controlled screw sense has fascinated a large number of scientists over the past two decades.²⁻⁴ These periodically structured materials contribute heavily to ingenious bio-functions such as genetic transfer, enzymatic reactions, antigen–antibody reactions, etc.⁵

Examples of such artificial helical structures are discotic amphiphilic molecules. Discotic amphiphilic molecules, for use in self-assembly, have a hydrophobic aromatic core tethered with flexible side chains.⁶⁻⁸ The strong π - π interactions between the π -conjugated cores make them prone to aggregate into supramolecular polymers e.g. columnar or helical aggregates.

In our research group, we are interested in studying the self-assembly behavior of conjugated aryltriazole amphiphilic molecules. These types of molecules are known to be planar,⁹ therefore we anticipated these types of molecules have the potential to stack and self-organize into higher order structures, stabilized by π - π interactions. This work will focus on the use of polar solvents to drive self-assembly by solvophobic forces. Solvophobicity can be an effective way to drive self-assembly of π -stacked structures into helical structures.^{10,11}

1.2 Aim

The aim of this work was to synthesize discotic amphiphilic materials bearing one and three chiral polar side chains respectively. We aimed to use spectroscopic- and microscopic characterization techniques to prove that helical architectures are present in their packing arrangement.

1.3 Structure of the thesis

A historical and theoretical background of discotic amphiphilic materials is given in Chapter 2. The potential self-assembly of these discotic amphiphiles into helical nano-structures is discussed. A few recent examples of these helical aggregates are given. In Chapter 3 the attempted synthesis of conjugated phenyl isoxazole dendrimers is discussed. Interest in

the isoxazole dendrimers systems has been frustrated by difficulties in obtaining the desired compounds. Therefore, an interesting alternative amphiphilic system with the potential to self-assemble into a helix was developed. Chapter 4 shows the synthesis and analysis of these amphiphilic materials. Self-assembly of these materials was investigated and is discussed. Final remarks and future work are discussed in Chapter 5.

1.4 References

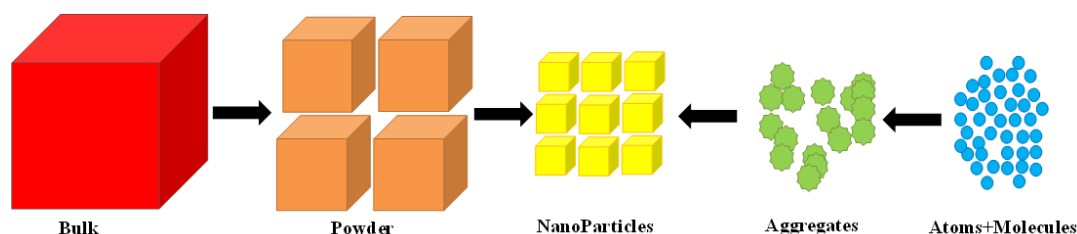
- (1) Block, M. A. B. *Folding Architectures Containing Phenylene Ethynylene Oligomers and Polymers*, 2006.
- (2) Banno, M.; Yamaguchi, T.; Nagai, K.; Kaiser, C.; Hecht, S.; Yashima, E. *J. Am. Chem. Soc.* **2012**, *134*, 8718–8728.
- (3) Ray, C. R.; S.Moore, J. *Adv. Polym. Sci.* **2005**, *177*, 91.
- (4) Hill, D. J.; Mio, M. J.; Prince, R. B.; Hughes, T. S.; Moore, J. S. *Chem. Rev. (Washington, DC, U. S.)* **2001**, *101*, 3893.
- (5) Ishihara, S.; Furuki, Y.; Takeoka, S. *Polym. Adv. Technol.* **2008**, *19*, 1097.
- (6) Kastler, M.; Pisula, W.; Wasserfallen, D.; Pakula, T.; Mullen, K. *J. Am. Chem. Soc.* **2005**, *127*, 4286.
- (7) Brunsveld, L.; Folmer, B. J. B.; Meijer, E. W.; Sijbesma, R. P. *Chem. Rev. (Washington, DC, U. S.)* **2001**, *101*, 4071.
- (8) Besenius, P.; Portale, G.; Bomans, P. H. H.; Janssen, H. M.; Palmans, A. R. A.; Meijer, E. W. *Proc. Natl. Acad. Sci. USA* **2010**, *107*, 17888.
- (9) Juricek, M.; Felici, M.; Contreras-Carballada, P.; Lauko, J.; Bou, S. R.; Kouwer, P. H. J.; Brouwerb, A. M.; Rowan, A. E. *J. Mater. Chem.* **2011**, *21*, 2104.
- (10) Lahiri, S.; Thompson, J. L.; Moore, J. S. *J. Am. Chem. Soc.* **2000**, *122*, 11315.
- (11) Zhao, D.; Moore, J. S. *Chem. Commun. (Cambridge, U. K.)* **2003**, 807.

Chapter 2 Self-Assembly and Packing of π -Conjugated Amphiphilic Materials

The creation of nanometer-scale (nanoscale) materials has fascinated and inspired the scientific community for more than a quarter of a century because of the wide range of applications of these materials e.g. applications in drug delivery, medicine, tissue engineering, memory storage, display and audio devices, semiconductors, etc.¹⁻⁷ Nanoscale aggregates are believed to be the future of constructing new ultra-miniaturised components for use in computational, electronic and optical devices.^{8,9} Other potential areas for nanostructures include: components in microsensors, basis for new classes of micelles and colloids; functional components in polymers; and catalysts or recognition elements.⁵ Nanostructures include the production and application of physical, chemical, and biological systems at scales ranging from individual atoms or molecules to submicron dimensions, as well as the integration into larger systems.^{3,10}

Synthesis of nano materials is commonly thought of in “top-down” and “bottom-up” processes (Scheme 2.1).^{1,11,12} Top-down approaches involve the modification of large aggregates that are cut and shaped by externally controlled tools into the desired shapes or structures; much like a sculpture is created out of a piece of rock.¹ The bottom-up approach is based on the principle of simple chemical building blocks self-organizing into large aggregates of molecules. This approach promises a better chance to obtain nano structures with less defects and more homogeneous chemical composition.^{1,10}

Scheme 2.1. Schematic representation of the top-down (left to right) and bottom-up approaches (right to left) towards nanostructures.



Biological systems primarily use the bottom-up approach to assemble e.g. proteins, DNA double helix, etc.¹³ DNA is a macromolecular polymer made up of small building blocks called nucleotides. These building blocks are composed of three

parts: a phosphate group, a deoxyribose sugar group and one of four types of nitrogen bases (adenine (A), thymine (T), guanine (G) and cytosine(C)). Nucleotides are linked into long polymeric chains called polynucleotides. A ladder like structure is formed when two polynucleotide chains are linked together by hydrogen bonds between base pairs. This ladder-like structure twists around an axis causing the molecule to form a double helix.^{13,14}

Scientists are constantly trying to simplify the tedious and repetitive nature of chemical syntheses as much as possible. A vast amount of research has gone into the development of systems in which low molar mass compounds autonomously assemble to produce large, ordered, aggregates. By understanding the size, shape, symmetry, and electronic properties of the binding sites on the molecular building blocks, the self-assembly of these supramolecular complexes can be easily manipulated.⁸ Self-assembly, which can also be classified as supramolecular polymerization,² is a popular phenomenon observed in various areas of the natural sciences namely, chemistry, physics, and biology. In supramolecular polymerization, the interactions between the building blocks are generated by reversible non-covalent interactions, resulting in high molecular weight linear polymers.^{2,3,15} Supramolecular polymerizations are categorized by three principles: (1) the physical nature of the non-covalent forces used, (2) the type of monomers used, and (3) the Gibbs free energy of the polymer as a function of conversion.¹⁵ Examples of these non-covalent interactions include: hydrogen bonds, π - π interactions, hydrophobic interactions, or metal-ligand binding.¹⁵

Biological systems provide numerous examples of the benefits of self-assembly, compared to artificial top-down approaches. An elegant example of a self-assembled biological system is the helical virus particle, the tobacco mosaic virus (TMV) (Figure 2.1a).^{1,5,8,16} The viral particle is composed of protein subunits, each containing 158 amino acids, which form a helical sheath around a single strand of RNA. The mechanism of TMV assembly is complex. Protein subunits form a disk-shaped assembly (Figure 2.1b), which is transformed into a helical form (Figure 2.1c) by insertion of a loop of RNA into the central hole of the protein disk. Additional protein disks, each corresponding to two turns of the final helix, associate with the growing viral particle (Figure 2.1d and e) until assembly is complete. The assembly of TMV demonstrates the ability of biological systems to construct large, ordered molecular

and supramolecular arrays from small, relatively simple subunits by self-assembly. Such processes are responsible for the wide diversity of structure and function observed at both the cellular and subcellular levels in Nature.^{1,8} The way nature has mastered the art of ordering large numbers of molecules into functional systems remains unmatched.¹⁴

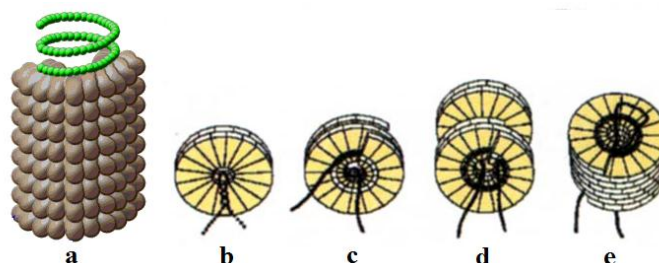


Figure 2.1. (a) The structure of the tobacco mosaic virus, (b)-(e) Self-assembly of the tobacco mosaic virus.¹

2.1 Helical Self-Assembly

The helix is an interesting motif that is one of the most frequently occurring secondary structural motifs used in nature.¹⁷ Synthesis of artificial helical structures with a controlled screw sense has fascinated a large number of scientists over the past two decades.¹⁸⁻²⁰ These periodically structured materials contribute heavily to ingenious bio-functions such as genetic transfer, enzymatic reactions, antigen–antibody reactions, etc.²¹ Examples (Figure 2.2) of different helices in nature includes the double stranded DNA (storing genetic information),¹³ the triple helical bundled collagen cable (providing mechanical strength in bone and tissue)²² as well as the gramicidin A channel (selectively allowing chemicals through cell membranes).^{17,23,24}

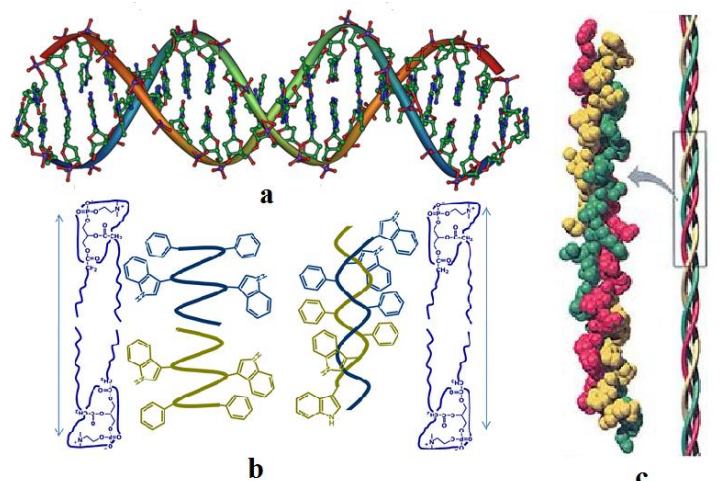
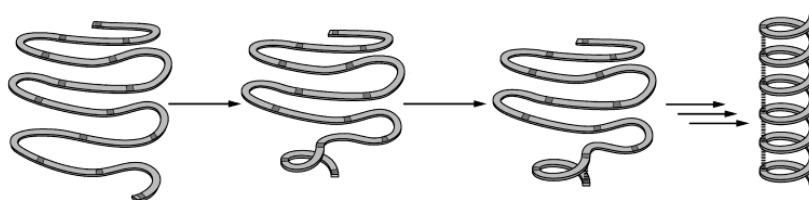


Figure 2.2. Helical motifs in Nature: (a) the DNA double helix, (b) open and closed gramicidin A channels²⁵ and (c) the triple helix of collagen.

Foldamers are an example of artificial helical architectures synthesized to self-organize into functional materials.^{19,20,26} They are defined as any polymers or oligomers that fold into a conformationally ordered state in solution (Scheme 2.2). The structures are stabilized by non-covalent interactions between non-adjacent monomer units.²⁰ Moore and co-workers developed one of the most popular helical foldamer motifs more than a decade ago.¹⁹ They investigated *m*-phenylene ethynylene oligomers, bearing chiral and achiral side chains, with the ability to fold into a helical conformation in polar solvents driven by solvophobic forces. Folded structures were stabilized by π - π stacking interactions.^{19,27-29}

Scheme 2.2 Folding of a random coil into a helical foldamer.²⁰



Another synthetic approach for making helical structures is by self-assembly or “stacking” of flat discotic molecules. Flat conjugated discotic molecules bearing aliphatic side chains, stack on top of each other via π - π interactions (Section 2.1.1).³⁰ The packing arrangement of these molecules can be compared to propellers piled on top of each other (Figure 2.3) where the propellers represent the side chains. The helical motif is generated by the bulky side chains arranging themselves in an offset fashion towards each other in order to minimize steric interactions between them.³¹ The large body of work on this subject, reported in

literature, proves that the stacking and self-assembly of molecules into helical columns is a very interesting phenomenon (Figure 2.3).²⁶

An example of this phenomenon is provided in work by Dehm *et al.* involving the helical growth of semiconducting dye assemblies based on chiral perylene bisimide derivatives (Figure 2.3a). It was shown that perylene bisimide (PBI) derivatives containing chiral side chains afforded helical supramolecular structures.³² Meijer and co-workers investigated the well-known benzene-1,3,5-tricarboxamide derivatives (Figure 2.3b).^{28,33,34} They managed to self-assemble these discotic molecules into helical, columnar aggregates of controlled length and cooperativity.²⁸ It was shown that the presence, or absence, of cooperativity in the self-assembly mechanism is very important in manipulating the physical properties of synthetic supramolecular polymers.³⁵ Other similar examples, by Meijer and co-workers, include the oligo(*p*-phenylenevinylene) derivatives (OPV) with chiral side chains, capped on one end by a tridodecyloxybenzene and on the other end by a ureidotriazine (Figure 2.3c),³⁶ discotic triamides (Figure 2.3d),³⁴ and bipyridine-based molecules (Figure 2.3e).³⁷ It was observed that the packing of the chiral side chains promoted the amplification of helical columnar assemblies.²¹

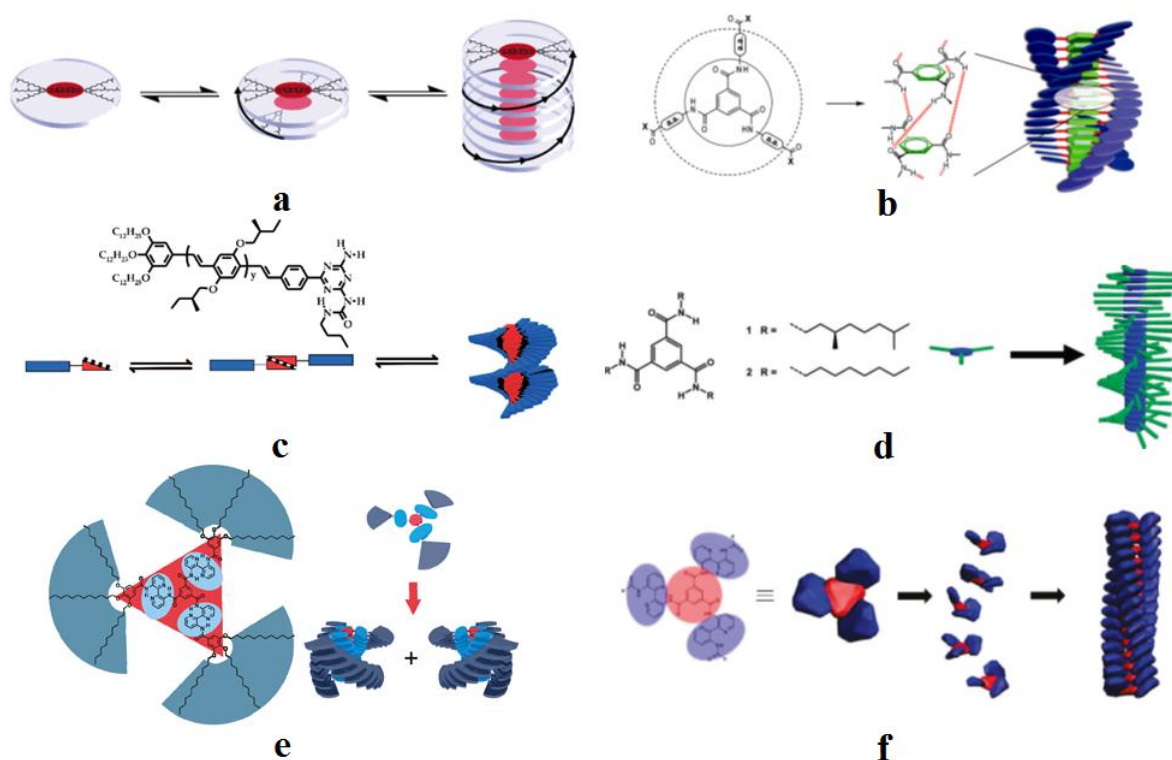


Figure 2.3. Examples of reported helical motifs; (a) Helical growth of chiral perylene bisimides,³² (b) Benzene-1,3,5-tricarboxamide core directs self-assembly into a helical architectures,²⁸ (c) Self-assembly of OPV derivatives,³⁶ (d) Self-assembly of discotic triamides,³⁴ (e) Self-assembly of bipyridine-based

molecules forming left- and right-handed helices,³⁷ (f) Self-assembly of twisted stacks of *N,N,N'*-tris[3(3'-carbamoylamino)-2,2'-bipyridyl]-benzene-1,3,5-tricarbonamide derivatives.¹¹

Danila *et al.* synthesized *N,N,N'*-tris[3(3'-carbamoylamino)-2,2'-bipyridyl]-benzene-1,3,5-tricarbonamide derivatives (Figure 2.3f) and studied their self-assembly. They also assessed the potential of the materials for use in electronic devices.¹¹ This demonstrated the potential for forming nanometer-sized fiber-like networks from small molecules, with a wide variety of applications.^{9,38-40} Columnar stacking of discotic liquid crystals (DLCs) have been utilized in opto-electronic devices owing to their advantageous properties including long-range self-assembly, ease of processing, solubility in a variety of organic solvents, and high charge-carrier mobilities along the π -stacked axis.⁴¹ In addition, the helical columnar liquid crystals offer promising scaffolds in the construction of helical nano-porous polymers via template polymerization.²¹ These approaches are enabling scientists to create new and highly ordered functional molecules from low molar mass molecules.⁴²

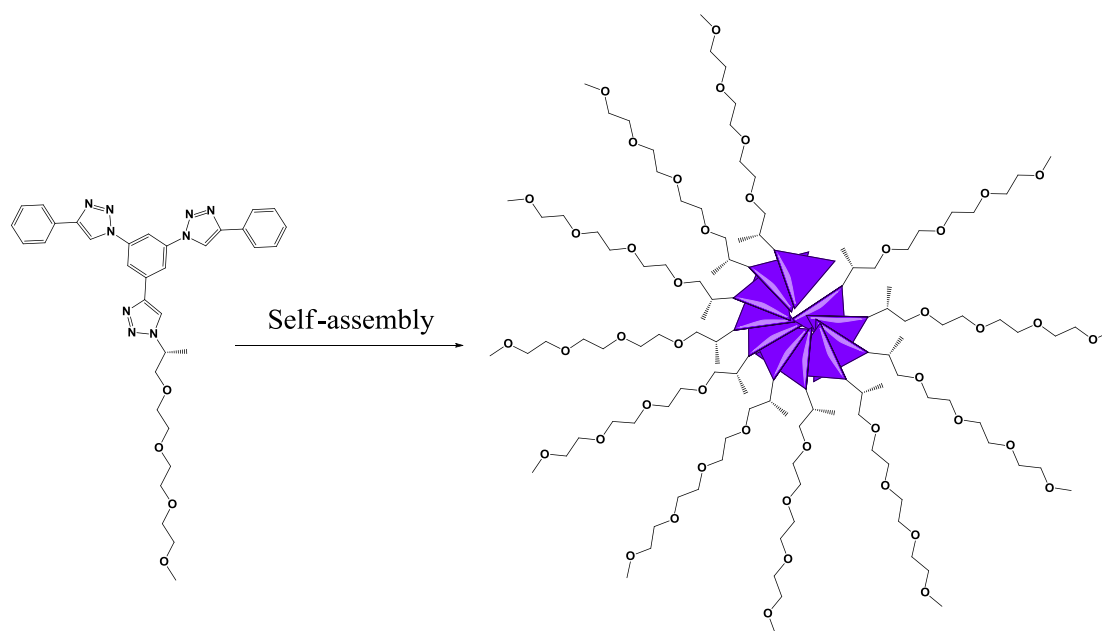
Helical Self-Assembly of Conjugated Discotic Amphiphiles

Discotic molecules, for use in self-assembly, have a similar design. Often these include a hydrophobic aromatic core, tethered with flexible side chains.^{26,28,43} The strong π - π interactions of the π -conjugated cores make them prone to aggregate into supramolecular polymers e.g. columnar or helical aggregates.²⁶ In some cases the role of the side chain is just to solubilize the molecule.⁴⁴ In amphiphilic systems the hydrophobic aromatic core and polar side chains instigate stacking by solvophobic forces.^{9,26,44} Discotic molecules are intriguing because of their electronic properties and their interesting controllable supramolecular structures. The π - π interactions within the stacked columns lead to high electron mobilities, which is necessary in the field of photovoltaics and plastics transistors.²⁶

In our research group, we are interested in studying the self-assembly behavior of conjugated aryltriazole molecules (Scheme 2.3). These types of molecules are known to be planar,⁴⁵ therefore we anticipated these types of molecules have the potential to stack and self-organize into higher order structures, stabilized by π - π interactions. One of the main advantages of using triazole containing molecules is that the triazoles can be synthesized easily and built into a variety of structures.⁴⁵ Triazoles are obtained by making use of the highly efficient copper-catalysed azide-alkyne cycloaddition⁴⁶, which is a "click-reaction".^{45,47} The conjugated triazole

containing molecules we were interested in do not resemble discotic molecules entirely because they do not have any side chains to give them an amphiphilic character therefore they do not have a great potential to self-assemble into helical aggregates. Modifying them with polar aliphatic side chains, e.g. polyethylene glycol, will give them an amphiphilic character with the potential to form helical aggregates.

Scheme 2.3. Schematic of potential self-assembly arytriazole amphiphiles with chiral side chains (purple triangle represents the π -conjugated core).



There are a number of factors that control the ability of discotic amphiphiles to self-assemble into ordered aggregates. These factors include temperature, solvent quality, concentration, monomer functionality, etc.⁴⁸ Other important factors include the potential to form π - π stacking interactions and chirality.^{36,48}

2.1.1 π - π Stacking

Studies on the self-assembly of π -conjugated discotic molecules have shown that these molecules “stack” on top of each other.^{9,32,39,49} Non-covalent interactions play a big role in stabilizing the stacks of discotic molecules.³⁰ This self-assembly into stacks represents a thermodynamic process, where the cofacial π - π stacking between the flat conjugated part of the molecules must override the lateral association caused by the hydrophobic interaction among the side chains.⁹ Lateral association involves the aggregation of side chains of these big molecules. When lateral interactions are favored over π - π interactions, the molecules align themselves up “next” to each other to maximize the side chain contact with adjacent molecules and hence do not pack into columns or helices.⁹

The strength of π - π stacking interactions has been found to depend strongly on solvent polarity, most likely due to the solvophobic nature of the aggregation (Section 2.1.3)⁵⁰ and the size of the conjugated aromatic surface.⁵¹ π -Conjugated molecules with large flat aromatic surfaces have stronger attractive forces between them.^{40,52} Another factor influencing the π - π stacking of discotic molecules is steric hindrance emanating from the side chains attached to the discotic core. This can perturb the disks from approaching one another.⁴³

Phenyl acetylene macrocycles are good examples of flat π -conjugated aromatic systems (Figure 2.4a).^{26,30,44,50,52} The ability of phenyl acetylene macrocycles to form stacks, stabilized by π - π stacking interactions, has been well documented.⁵² Moore and co-workers studied the self-assembly of these macrocycles by applying the electrostatic theory of π - π interactions and the dimerization studies of these molecules, they were able to insert electron-withdrawing functionalities on the side chains (Figure 2.4a).⁵²

Recently the potential of tetrathiafulvalene macrocycles (Figure 2.4b), to form supramolecular structures, has been examined.⁵³ These macrocycles did not assemble in chloroform and tetrahydrofuran (THF), and formed dimers in toluene, but assembled in aqueous THF solutions.⁵⁴ This was attributed to hydrophobic interactions.⁵⁴

Hexa-peri-hexabenzocoronenes (HBC) (Figure 2.4c) are another example of flat discotic materials that tend to self-assemble in bulk forming large clusters of stacked columns.^{41,43,55,56} HBCs are graphene derivatives which possess a π -conjugated core and are solubilized by aliphatic side chains tethered to their periphery (Figure 2.4c).³⁵ Extensive research has been carried out to understand their packing in the liquid crystalline state.⁴³ Their self-assembly in the bulk and on surfaces has been studied by different techniques such as X-ray diffraction and scanning probe microscopy.⁵⁵ HBCs are unique in that they stack without a screw sense, forming columns instead of helices (Figure 2.4c). Note that all the HBC side chains are achiral. This, however, does not mean that the side chains have to be chiral to form helices. Percec *et al.* recently constructed a similar type of self-assembled suprastructure using a rigid aromatic core bearing a dendronized "side chain" (Figure 2.4d).⁵⁷ This self-assembly was apparently driven by electrostatic interactions between electron-withdrawing nitrile groups and electron-donating phenoxy groups.

Consequently, the conjugated core is faced inwards while the side chains are assembled on the outside of the columns. These structures are stabilized by π - π interactions.⁵⁷

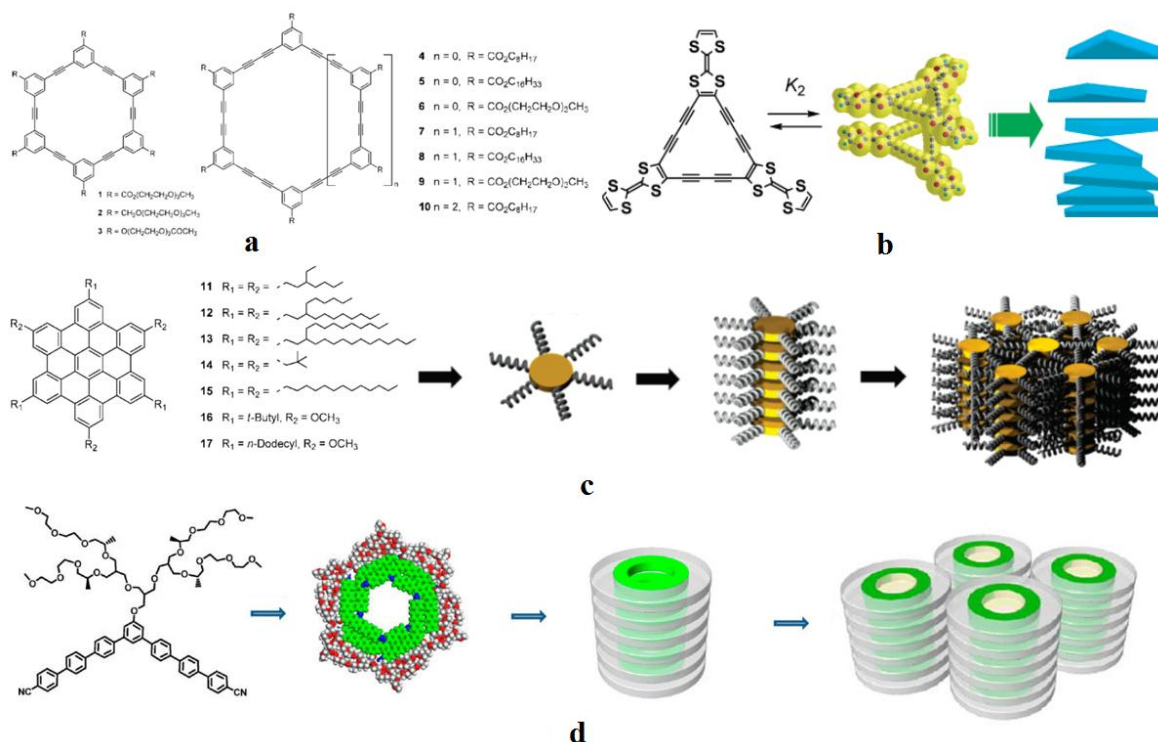
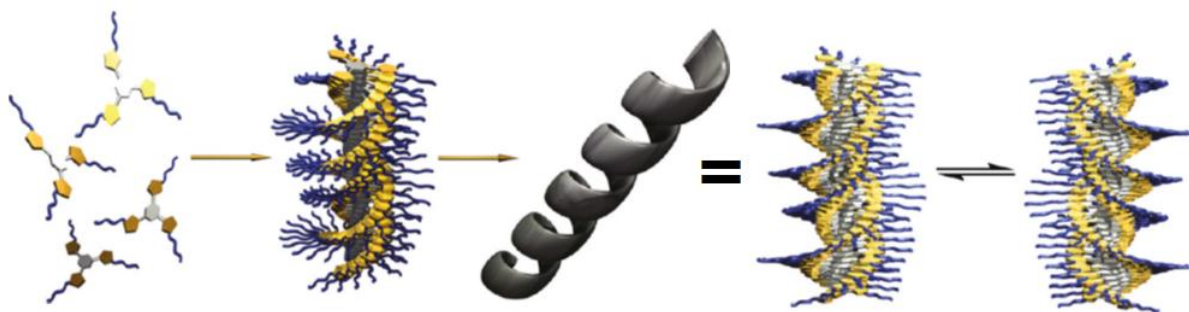


Figure 2.4. Examples of systems which form π - π stacking interactions in self-assembly: (a) Phenyl acetylene macrocycles,⁵² (b) Tetrathiafulvalene macrocycles,⁵⁴ (c) Hexa-peri-hexabenzocoronenes' chemical structure and a schematic of their self-assembly into columns and aggregates,⁵⁸ (d) Schematic representation of proposed self-assembly for formation of hexameric macrocycles.⁵⁷

As mentioned in Section 2.1 (Figure 2.3), there are many examples of discotic amphiphilic molecules that assemble into helical motifs. The helical motif is obtained when a discotic molecule stacks on top of the previous molecule with a slight off-set compared to that molecule. An example of achiral amphiphilic molecules that have the ability to form helical stacks are the tris(phenylisoxazolyl)benzenes (Scheme 2.4).⁴⁰ Haino *et al.* showed that these discotic molecules can form helices without having chiral side chains.⁴⁰ Their self-assembly was investigated using ^1H NMR and UV-vis spectroscopy. It was observed via ^1H NMR spectroscopy, that the signals of the aromatic protons shift upfield with increasing concentrations. This suggests the formation of stacked assemblies, which place the aromatic protons into shielding regions produced by the neighboring aromatic rings.⁴⁰

Scheme 2.4. Self-assembly of tris(phenylisoxazolyl)benzene into helical structures showing the equilibrium between left- and right handed helices.⁴⁰



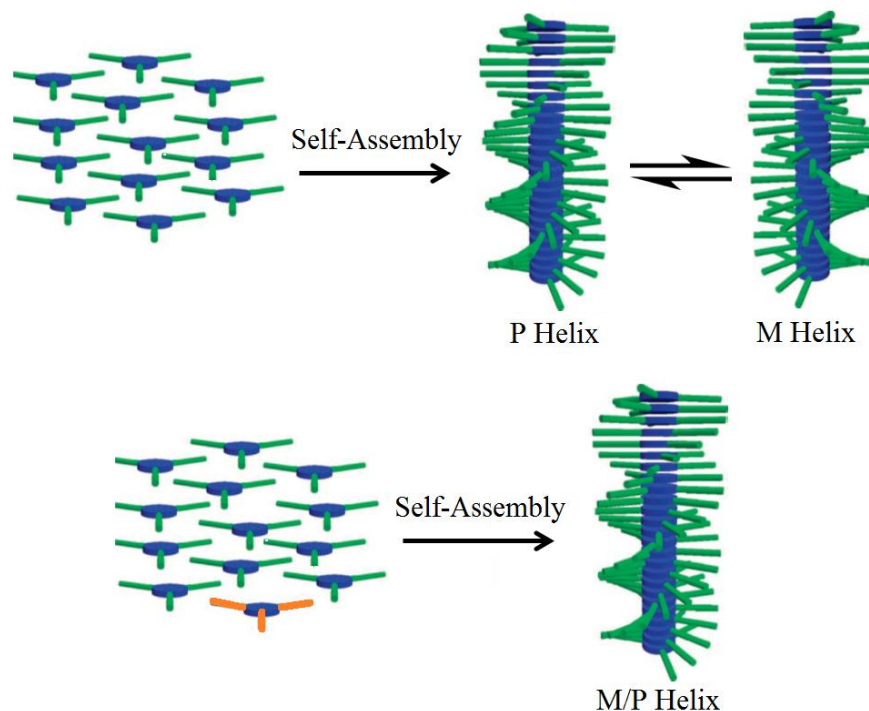
When achiral side chains were attached to the conjugated aromatic core the resulting helical structures had both left- and right handed helical conformations (M and P helices). The result was a racemic mixture of two enantiomers (Scheme 2.4). This equilibrium was biased to either left- or right handed helical assemblies by the attachment of chiral enantiopure side chains to the conjugated aromatic core (Section 2.1.2).⁴⁰ This phenomenon is called chiral amplification.

2.1.2 Chiral Amplification of Discotic Molecules

Chiral amplification in the monomeric components of polymers found in biological and natural systems plays a big role in the biological function, especially with respect to the folding and hierarchical self-assembly into large functional nano materials.⁵⁹ Chiral amplification is a very challenging topic of discussion in the field of chemistry, physics, and biology.^{39,59-61} Chirality is introduced to the amphiphilic system via the side chains attached to the conjugated core.⁴⁸ The helical self-assembly of discotic molecules that do not have elements of chirality, results in an equal amount of left- and right-handed helices being formed (Scheme 2.4).⁴⁰ This racemic mixture can be biased to one enantiomer by either using an enantiopure compound for self-assembly or by making use of the sergeants-and-soldiers principle (Scheme 2.5).^{31,34,39,62} Enantiomerically pure discotic amphiphiles will drive the stacking into single-handed helix, however it is relatively tedious and often costly to synthesize large amounts of enantiomerically pure materials. The sergeants-and-soldiers principle was developed to minimize the amount of chiral material necessary in order to form single-handed helices. It works on the principle that only a small amount of chiral amplification is necessary to drive a single handed helix formation.^{11,39,59} The introduction of a chiral source (small amount of a chiral molecule) to an achiral

monomer solution, drives the helix formation to the most favorable steric conformation.^{63,64}

Scheme 2.5. Schematic representation of the sergeants-and-soldiers principle. In the first scheme both M- and P-Helices are obtained because of achiral side chains, while the second scheme forms a single handed helix because of the addition of a chiral molecule (orange side chains).



Meijer and co-workers carried out extensive investigations on the sergeants-and-soldiers principle using discotic systems tethered with chiral and achiral side chains (Figure 2.5).³¹ X-ray diffraction showed that both chiral and achiral systems resulted in some degree of a helical superstructure. It was found that the molecules stacked in highly ordered chiral columns, with a strong cooperative response to chiral information.³¹ The achiral discotics formed both left- and right handed helices, whilst the chiral discotics formed a preferred screw sense. Consequently dilute solutions of the former gave very strong negative Cotton effects in the UV region associated with the π - π^* absorption band of the bipyridine moiety.³¹ It was observed that the mixtures of 1a and 1b generated strong Cotton effects, with positive deviation from linearity, affirming sergeants-and-soldiers behavior.³¹

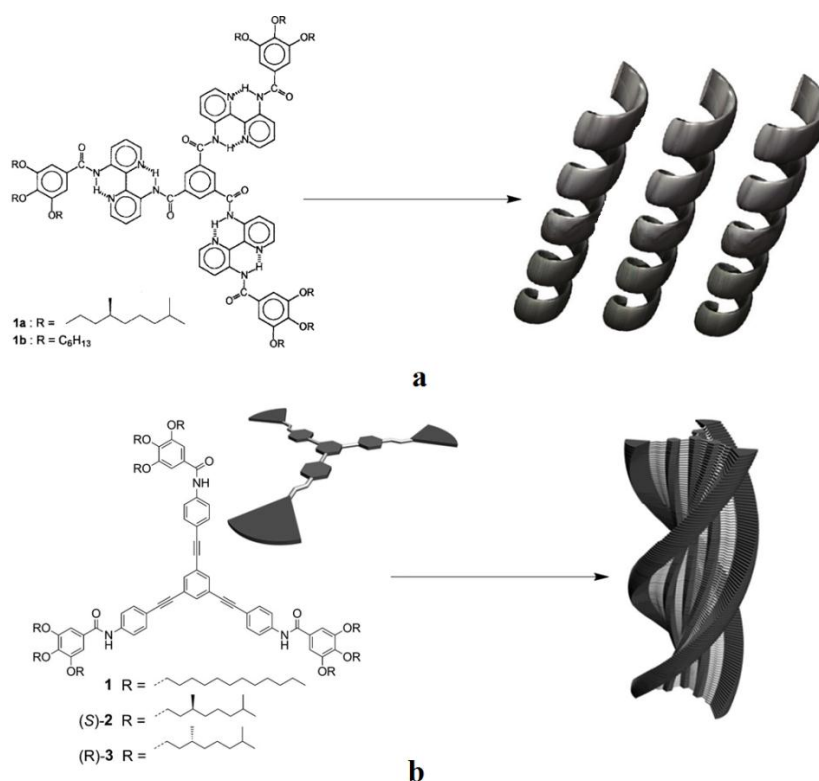


Figure 2.5. (a) Structure of discotic moieties, bearing either achiral or chiral side chains, for helical self-assembly,³¹ (b) Structures of discotic tris-amides and schematic representation of the supramolecular polymerisation process into helical stacks.⁶⁵

Recently the self-assembly of an interesting example of π -conjugated oligo(phenylene ethynylene) (OPE) discotic amphiphiles was investigated. The OPE was designed and synthesized so as to construct one-dimensional, helical, supramolecular polymers.⁶⁵ The presence of hydrogen-bonding and π - π stacking interactions in combination with solvophobic effects could induce the discotic tris-amides to self-assemble into elongated, columnar aggregates in solution. Chiral amplification studies on the C_3 -symmetrical OPEs revealed a very strong sergeants-and-soldiers effect.⁶⁵

2.1.3 Solvent effects

Solvent quality is one of the key ingredients in regulating the self-assembly of small organic molecules.^{55,62,66} Various studies on different solvents properties have been carried out to show their different effects on the self-assembly process. These properties include the influence of solvent chirality, polarity and the size of the solvent molecule.^{36,58} Solvent molecules play a definitive role in rigidifying the aggregates and guiding them toward further assembly into bundles or gels.³⁶ The type of solvent and the solvent structure is very important in the association process.

Solvent molecules can stabilize or destabilize the non-covalent interactions responsible for self-assembly. For example, benzene stabilizes π - π interactions.⁵⁸ The use of chiral solvents has been shown to induce a preferred handedness in supramolecular stacks.⁴⁸ Bulky solvents have also been shown to affect the close packing of molecules.⁴⁸

This work will focus on the use of polar solvents to drive self-assembly by solvophobic forces. Solvophobicity can be an effective way to drive self-assembly of π -stacked structures into helical structures.^{44,52} Solvophobicity involves the assistance of a “poor solvent” to drive molecules into well-defined structures.⁵⁰ In a “good solvent”, both the discotic conjugated core and the side chains are well-solvated. Use of a more polar solvent (“poor solvent”) causes a collapse/aggregation as the side chains are better solvated than the conjugated π -stacked backbone.⁵⁰ The hydrophobic core of the aggregates avoids contact with the polar solvent by forming columnar or helical stacks with polar side chains facing outward. These aggregations are also stabilized by the π -stacking of the aromatic framework and van der Waals interactions between the side chains.^{50,60} As solvophobic interactions have been demonstrated to favor aromatic stacking, the introduction of longer hydrophobic side chains onto the discotic core should further intensify the solvophobicity of the columnar or helical “backbone” in polar solvents and lead to stronger aggregation.^{26,52} The solvent does not play a distinctive role in the type of aggregation obtained *i.e.* columnar or helical formation. The nature of the monomers used in the system plays the biggest role in determining whether or not a helix will form. In most cases where chiral side chains are used, helical structures are obtained; however this does not mean that the side chains have to be chiral to form helical aggregates (Section 2.1.1).

Apolar solvents do not always differentiate between hydrogen bonding, π - π stacking and hydrophobic interactions responsible for aggregation. On the other hand, polar solvents can interfere with some secondary interactions.⁴² Polar solvents are either protic or aprotic, meaning they either can or cannot assist hydrogen bonding.⁶⁷ The most common protic solvents include water, alcohols, and carboxylic acids, whilst examples of aprotic solvents include dimethylformamide, dimethylsulfoxide, and acetonitrile. Amphiphilic discotic molecules are well-documented to self-assemble in aprotic solvents (“poor solvent”) because like previously mentioned, the non-polar

discotic core avoids contact with surrounding polar solvent by directing the aliphatic side chains outward. The solvophobic effect causes the discotic molecules to form columnar or helical aggregates containing a hydrophobic core.^{28,48} Practically, a popular method for effecting the hydrophobic effect involves the addition of water to a polar aprotic solvent.⁶⁸ The hydrophobic effect is the observed tendency of nonpolar substances (in this case the discotic core) to aggregate in aqueous solution and minimize contact with the surrounding water.¹⁴

2.2 Characterization of Self-assembled Helical Aggregates

Various techniques are used to characterize the well-defined structures of self-assembly. These techniques include nuclear magnetic resonance (NMR) spectroscopy, ultraviolet–visible spectroscopy (UV-Vis), microscopy, circular dichroism (CD) spectroscopy, vapor pressure osmometry (VPO), and dynamic light scattering (DLS), etc.^{27,30,60,69,70}

2.2.1 NMR-Spectroscopy

Nuclear magnetic resonance (NMR) spectroscopy is a very useful technique for showing the presence of self-assembled aggregates.^{42,49,52} In general, when two or more aromatic units come into close vicinity of each other, the nuclei of one molecule are affected by the ring-current magnetic anisotropy of the other.⁴⁰ This normally brings about an upfield shift in the resonance peaks of aromatic moieties involved in the self-assembly.^{43,52,71,72} In some cases it has been reported that with increasing concentration, the aromatic signals also show signs of broadening.⁴²

2.2.2 UV-Spectroscopy

The UV-vis spectra of self-assembled aggregates in solution, are often characterized by red shifts. This is usually considered as evidence for the formation of aggregates.^{28,31,38,42} Different variables in these experiments include concentration, temperature, and solvent composition. Aggregation is also suggested when UV-vis bands broaden and lose fine structure with increasing concentration.^{26,40}

2.2.3 Microscopy

Microscopy provides visual evidence of the formation of higher order structures. Definite evidence for successful control over one dimensional stack length can be obtained using different microscopic techniques.⁷³ These techniques include transmission electron microscopy (TEM), scanning electron microscopy (SEM), atomic force microscopy (AFM), and Scanning tunneling microscopy (STM).

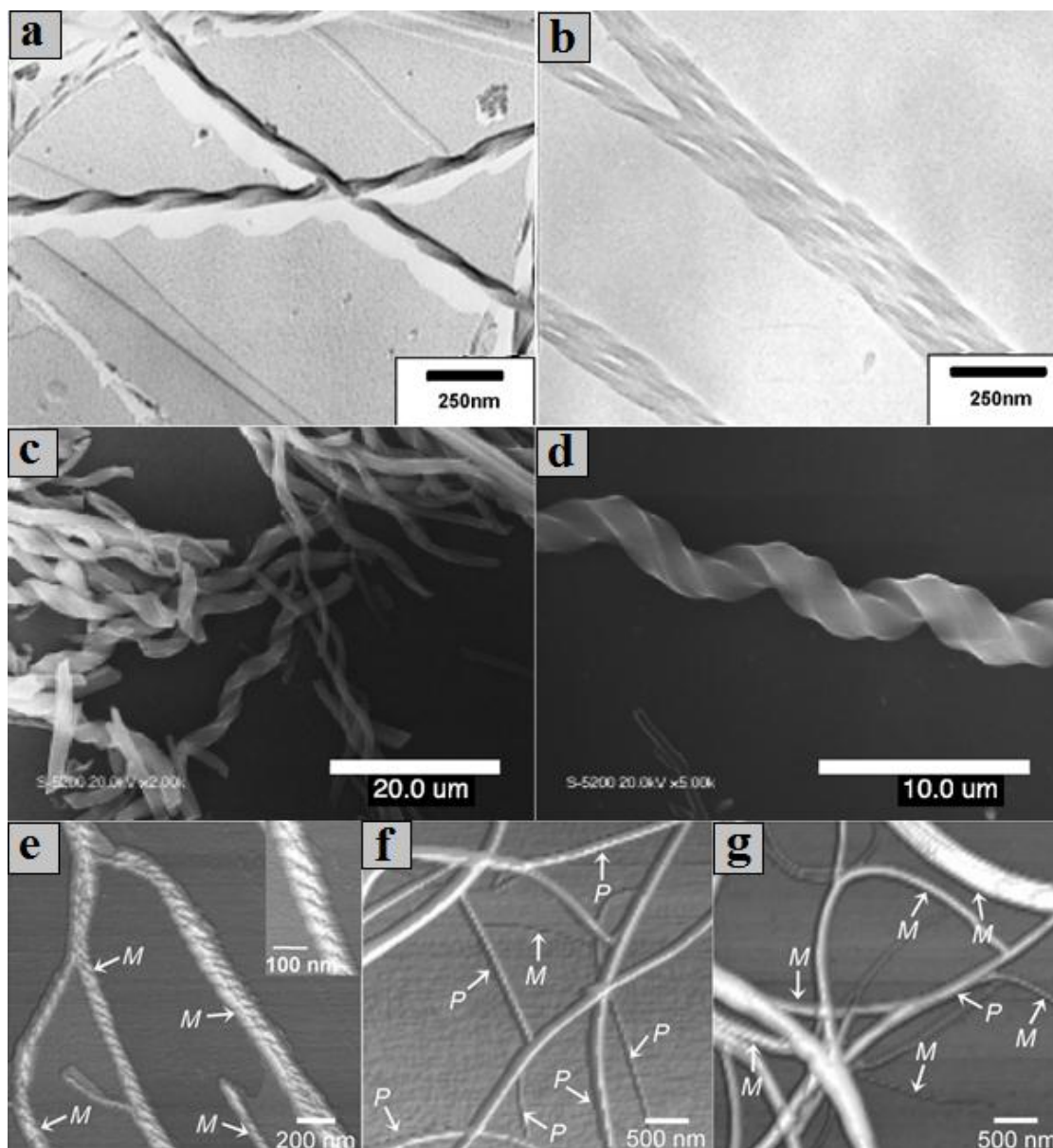


Figure 2.6. (a),(b) TEM images of helical ribbon nano structures from rod-coil block copolymers,⁷⁴ (c),(d) FESEM images of the xerogel of tris(phenylisoxazolyl)benzene derivative,⁴⁰ (e)-(f) shows AFM images of an oligo(*p*-phenylenevinylene) derivate: (e) homoassembly, (f) coassembly of the initial achiral derivative with 9% chiral derivative, (g) coassembly of initial achiral derivative with 60% chiral derivative.⁶⁶

The two electron microscopy techniques TEM and SEM are very useful to show the presence of self-assembled helical or columnar rods.^{60,69,73-75} TEM sample preparation has the drawback that structural morphology of some compounds can change while drying the sample before analysis. Cryogenic transmission electron microscopy (cryo-TEM) is advantageous over the conventional TEM in that the structural morphology of the self-assembled aggregates is preserved.²⁸ SEM is also a good technique to show aggregation had taken place. It is used to study the

texture, topography and surface of a sample.^{11,39,53} SEM scans the surface of the sample by releasing electrons and making the electrons bounce or scatter upon impact and then the scattered electrons are collected and an image produced (Figure 2.6c,d).¹¹ Field-emission scanning electron microscopy (FESEM) is a specific type of SEM. It holds a few advantages over its predecessor, e.g. it can observe the tilt and cross-sections, as well as analyze the elemental composition by the energy dispersive X-ray analysis.^{12,76} An example of a FESEM image of tris(phenylisoxazolyl)benzene derivatives (Figure 2.6c,d) shows a distinctive helical structure.⁴⁰ AFM is also a technique used to investigate the surface of samples. It is a type of scanning probe microscopy with a very high-resolution and is a very efficient method to prove the formation of helical self-assembled aggregates. Figure 2.6e-f are AFM images of oligo(p-phenylenevinylene) derivatives. M- and P helices are clearly visible in these pictures.⁶⁶

2.2.4 Circular Dichroism

Circular dichroism is a very powerful technique for determination of the secondary structure of molecules or aggregates. The technique works on the principle of unequal absorption of left and right handed circularly polarized light. CD detects diastereomeric excess.⁷⁷ This diastereomeric excess is shown by a change in optical rotation versus wavelength in the region of an absorption band also known as a Cotton-effect.

Figure 2.7a shows a typical CD-spectrum where a clear Cotton-effect can be seen. Here the self-assembly of a flavin derivative was studied at different temperatures in hexane.⁷¹ This proves that a helical structure is present. As previously mentioned, the aggregate can be biased to either assemble in a left- or right handed helix. This biasing of the screw sense can be shown by CD-spectroscopy. The spectrum of a left-handed helix will be inverted compared to the spectrum of the right handed helix of the same compound. Figure 2.7b shows a CD-spectrum of a left handed versus right handed helical structure.⁷¹

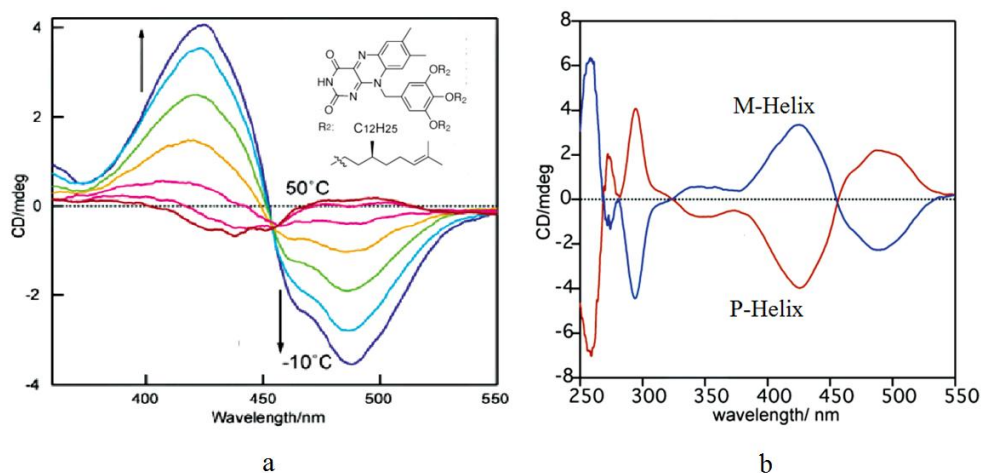


Figure 2.7. (a) Variable temperature CD spectra in hexane, (b) Mirror image Cotton-effects observed for M- and P-Helices.⁷¹

2.3 Approach

Conjugated phenyl-triazole dicotics tethered with chiral polar side chains have the potential to stack via π - π interactions. The chiral character of the polar side chains will possibly drive these discotics to stack into helices. Self-assembly of these discotic molecules via π - π interactions and solvophobic forces was investigated in this study and is discussed in Chapter 4.

2.4 References:

- (1) Philp, D.; Stoddart, J. F. *Angew. Chem., Int. Ed.* **1996**, *35*, 1154.
- (2) Bosman, A. W.; Sijbesma, R. P.; Meijer, E. W. *Mater. Today* **2004**, *7*, 34.
- (3) Cacialli, F.; Samorì, P.; Silva, C. *Mater. Today* **2004**, *7*, 24.
- (4) Hecht, S. *Mater. Today* **2005**, *8*, 48.
- (5) Whitesides, G. M.; Mathias, J. P.; Seto, C. T. *Science* **1991**, *254*, 1312.
- (6) Lehn, J.-M. *Science* **2002**, *295*, 2400.
- (7) Hristozov, D.; Ertel, J. *Forum der Forschung* **2009**, *22*, 161.
- (8) Steed, J. W.; Atwood, J. L. *Supramolecular chemistry*; Wiley, 2000.
- (9) Zang, L.; Che, Y.; Moore, J. S. *Acc. Chem. Res.* **2008**, *41*, 1596.
- (10) Bhushan, B. *Springer Handbook of Nanotechnology*; Springer, 2006.
- (11) Danila, I.; Riobe, F.; Piron, F.; Puigmartí-Luis, J.; Wallis, J. D.; Linares, M.; Ågren, H.; Beljonne, D.; Amabilino, D. B.; Avarvari, N. *J. Am. Chem. Soc.* **2011**, *133*, 8344.
- (12) John, G.; Jung, J. H.; Minamikawa, H.; Yoshida, K.; Shimizu, T. *Chem. Eur. J.* **2002**, *8*, 5494.
- (13) Watson, J. D.; Crick, F. H. C. *Nature* **1953**, *171*, 737.
- (14) Hoeben, F. J. M.; Jonkheijm, P.; Meijer, E. W.; Schenning, A. P. H. J. *Chem. Rev. (Washington, DC, U. S.)* **2005**, *105*, 1491.
- (15) Smulders, M. M. J.; Nieuwenhuizen, M. M. L.; Greef, T. F. A. d.; v. d. Schoot, P.; Schenning, A. P. H. J.; Meijer, E. W. *Chem. Eur. J.* **2010**, *16*, 362
- (16) Lindsey, J. S. *New J. Chem.* **1991**, *15*, 153.
- (17) Block, M. A. B. *Folding Architectures Containing Phenylene Ethynylene Oligomers and Polymers*, 2006.
- (18) Banno, M.; Yamaguchi, T.; Nagai, K.; Kaiser, C.; Hecht, S.; Yashima, E. *J. Am. Chem. Soc.* **2012**, *134*, 8718–8728.
- (19) Ray, C. R.; S. Moore, J. *Adv. Polym. Sci.* **2005**, *177*, 91.
- (20) Hill, D. J.; Mio, M. J.; Prince, R. B.; Hughes, T. S.; Moore, J. S. *Chem. Rev. (Washington, DC, U. S.)* **2001**, *101*, 3893.
- (21) Ishihara, S.; Furuki, Y.; Takeoka, S. *Polym. Adv. Technol.* **2008**, *19*, 1097.
- (22) Yu, S. M.; Lib, Y.; Kim, D. *Soft Matter* **2011**, *7*, 7927.
- (23) Kelkar, D. A.; Chattopadhyay, A. *Biochim. Biophys. Acta* **2007**, *1768*, 2011.
- (24) Katsaras, J.; Prosser, R. S.; Stinson, R. H.; Davis, J. H. *Biophys. J.* **1992**, *61*, 827.
- (25) Halder, S.; Chaudhuri, A.; Gu, H.; Koeppe, R. E.; Kombrabail, M.; Krishnamoorthy, G.; Chattopadhyay, A. *J. Phys. Chem. B* **2012**, *116*, 11056–11064.
- (26) Brunsveld, L.; Folmer, B. J. B.; Meijer, E. W.; Sijbesma, R. P. *Chem. Rev. (Washington, DC, U. S.)* **2001**, *101*, 4071.
- (27) Meng, Q.; Kou, Y.; Ma, X.; Liang, Y.; Guo, L.; Ni, C.; Liu, K. *Langmuir* **2012**, *28*, 5017.
- (28) Besenius, P.; Portale, G.; Bomans, P. H. H.; Janssen, H. M.; Palmans, A. R. A.; Meijer, E. W. *Proc. Natl. Acad. Sci. USA* **2010**, *107*, 17888.
- (29) Ronis, D.; Martina, E.; Deutch, J. M. *Chem. Phys. Lett.* **1977**, *46*, 53.
- (30) Shetty, A. S.; Zhang, J.; Moore, J. S. *J. Am. Chem. Soc.* **1996**, *118*, 1019.
- (31) Palmans, A. R. A.; Vekemans, J. A. J. M.; Havinga, E. E.; Meijer, E. W. *Angew. Chem., Int. Ed. Engl.* **1997**, *36*, 2648.
- (32) Dehm, V.; Chen, Z.; Baumeister, U.; Prins, P.; Siebbeles, L. D. A.; Wurthner, F. *Org. Lett.* **2007**, *9*, 1085.
- (33) Hout, K. P. v. d.; Martin-Rapun, R.; Vekemans, J. A. J. M.; Meijer, E. W. *Chem. Eur. J.* **2007**, *13*, 8111
- (34) Smulders, M. M. J.; Schenning, A. P. H. J.; Meijer, E. W. *J. Am. Chem. Soc.* **2008**, *130*, 606.

- (35) Greef, T. F. A. D.; Smulders, M. M. J.; Wolffs, M.; Schenning, A. P. H. J.; Sijbesma, R. P.; Meijer, E. W. *Chem. Rev. (Washington, DC, U. S.)* **2009**, *109*, 5687.
- (36) Jonkheijm, P.; Schoot, P. v. d.; Schenning, A. P. H. J.; Meijer, E. W. *Science* **2006**, *313*, 80.
- (37) Martin-Rapun, R.; Byelov, D.; Palmans, A. R. A.; Jeu, W. H. d.; Meijer, E. W. *Langmuir* **2009**, *25*, 8794.
- (38) Herrikhuyzen, J. v.; Syamakumari, A.; Schenning, A. P. H. J.; Meijer, E. W. *J. Am. Chem. Soc.* **2004**, *126*, 10021.
- (39) Ishi-i, T.; Kuwahara, R.; Takata, A.; Jeong, Y.; Sakurai, K.; Mataka, S. *Chem. Eur. J.* **2006**, *12*, 763.
- (40) Tanaka, M.; Ikeda, T.; Mack, J.; Kobayashi, N.; Haino, T. *J. Org. Chem.* **2011**, *76*, 5082.
- (41) Kaafarani, B. R. *Chem. Mater.* **2011**, *23*, 378.
- (42) Brunsveld, L.; Zhang, H.; Glasbeek, M.; Vekemans, J. A. J. M.; Meijer, E. W. *J. Am. Chem. Soc.* **2000**, *122*, 6175.
- (43) Kastler, M.; Pisula, W.; Wasserfallen, D.; Pakula, T.; Mullen, K. *J. Am. Chem. Soc.* **2005**, *127*, 4286.
- (44) Lahiri, S.; Thompson, J. L.; Moore, J. S. *J. Am. Chem. Soc.* **2000**, *122*, 11315.
- (45) Juricek, M.; Felici, M.; Contreras-Carballada, P.; Lauko, J.; Bou, S. R.; Kouwer, P. H. J.; Brouwerb, A. M.; Rowan, A. E. *J. Mater. Chem.* **2011**, *21*, 2104.
- (46) Tornøe, C. W.; Christensen, C.; Meldal, M. *J. Org. Chem.* **2002**, *67*, 3057.
- (47) Rostovtsev, V. V.; Green, L. G.; Fokin, V. V.; Sharpless, K. B. *Angew. Chem., Int. Ed.* **2002**, *41*, 2596.
- (48) Nakano, Y.; Hirose, T.; Stals, P. J. M.; Meijer, E. W.; Palmans, A. R. A. *Chem. Sci.* **2012**, *3*, 148.
- (49) Cubberley, M. S.; Iverson, B. L. *J. Am. Chem. Soc.* **2001**, *123*, 7560.
- (50) Kubel, C.; Mio, M. J.; Moore, J. S.; Martin, D. C. *J. Am. Chem. Soc.* **2002**, *124*, 8605.
- (51) Nolde, F.; Pisula, W.; Muller, S.; Kohl, C.; Mullen, K. *Chem. Mater.* **2006**, *18*, 3715.
- (52) Zhao, D.; Moore, J. S. *Chem. Commun. (Cambridge, U. K.)* **2003**, 807.
- (53) Danila, I.; Pop, F.; Escudero, C.; Feldborg, L. N.; Puigmarti-Luis, J.; Riobe, F.; Avarvari, N.; Amabilino, D. B. *Chem. Commun. (Cambridge, U. K.)* **2012**, *48*, 4552.
- (54) Enozawa, H.; Hasegawa, M.; Takamatsu, D.; Fukui, K.-i.; Iyoda, M. *Org. Lett.* **2006**, *8*, 1917.
- (55) Samori, P.; Yin, X.; Tchebotareva, N.; Wang, Z.; Pakula, T.; Jackel, F.; Watson, M. D.; Venturini, A.; Mullen, K.; Rabe, J. P. *J. Am. Chem. Soc.* **2004**, *126*, 3567.
- (56) Bhattacharya, S.; Samanta, S. K. *Langmuir* **2009**, *25*, 8378.
- (57) Kim, H.-J.; Liu, F.; Ryu, J.-H.; Kang, S.-K.; Zeng, X.; Ungar, G.; Lee, J.-K.; Zin, W.-C.; Lee, M. *J. Am. Chem. Soc.* **2012**, *134*, 13871.
- (58) Wu, J.; Pisula, W.; Mullen, K. *Chem. Rev. (Washington, DC, U. S.)* **2007**, *107*, 718.
- (59) Wilson, A. J.; Masuda, M.; Sijbesma, R. P.; Meijer, E. W. *Angew. Chem.* **2005**, *117*, 2315.
- (60) García, F.; Aparicio, F.; Marenchino, M.; Campos-Olivas, R.; Sánchez, L. *Org. Lett.* **2010**, *12*, 4264.
- (61) Lee, S. J.; Kim, E.; Seo, M. L.; Do, Y.; Lee, Y.-A.; Lee, S. S.; Jung, J. H.; Kogiso, M.; Shimizu, T. *Tetrahedron* **2008**, *64*, 1301.

- (62) Smulders, M. M. J.; Filot, I. A. W.; Leenders, J. M. A.; Schoot, P. v. d.; Palmans, A. R. A.; Schenning, A. P. H. J.; Meijer, E. W. *J. Am. Chem. Soc.* **2010**, *132*, 611.
- (63) Cantekin, S.; Eikelder, H. M. M. t.; Markvoort, A. J.; Veld, M. A. J.; Korevaar, P. A.; Green, M. M.; Palmans, A. R. A.; Meijer, E. W. *Angew. Chem., Int. Ed.* **2012**, *51*, 6426.
- (64) Cat, I. D.; Guo, Z.; George, S. J.; Meijer, E. W.; Schenning, A. P. H. J.; Feyter, S. D. *J. Am. Chem. Soc.* **2012**, *134*, 3171.
- (65) Wang, F.; Gillissen, M. A. J.; Stals, P. J. M.; Palmans, A. R. A.; Meijer, E. W. *Chem. Eur. J.* **2012**, *18*, 11761.
- (66) Ajayaghosh, A.; Varghese, R.; George, S. J.; Vijayakumar, C. *Angew. Chem., Int. Ed.* **2006**, *45*, 1141.
- (67) Wypych, G. *Handbook of Solvents*; ChemTec, 2001.
- (68) Hirose, T.; Irie, M.; Matsuda, K. *Chem. Asian J.* **2009**, *4*, 58.
- (69) Messmore, B. W.; Hulvat, J. F.; Sone, E. D.; Stupp, S. I. *J. Am. Chem. Soc.* **2004**, *126*, 14452.
- (70) Schaefer, C.; Voets, I. K.; Palmans, A. R. A.; Meijer, E. W.; Schoot, P. v. d.; Besenius, P. *ACS Macro Lett.* **2012**, *1*, 830.
- (71) Nakade, H.; Jordan, B. J.; Xu, H.; Han, G.; Srivastava, S.; Arvizo, R. R.; Cooke, G.; Rotello, V. M. *J. Am. Chem. Soc.* **2006**, *128*, 14924.
- (72) Chang, K.-J.; Kang, B.-N.; Lee, M.-H.; Jeong, K.-S. *J. Am. Chem. Soc.* **2005**, *127*, 12214.
- (73) Flanningani, D. J.; Zewail, A. H. *Acc. Chem. Res.* **2012**, *45*, 1828.
- (74) Sung, C.-H.; Kung, L.-R.; Hsu, C.-S.; Lin, T.-F.; Ho, R.-M. *Chem. Mater.* **2006**, *18*, 352.
- (75) Olsen, B. D.; Segalman, R. A. *Mater. Sci. Eng. R Rep.* **2008**, *62*, 37.
- (76) Zhu, Y. Y.; Ding, G. Q.; Ding, J. N.; Yuan, N. Y. *Nanoscale Res. Lett.* **2010**, *5*, 725.
- (77) Berova, N.; Nakanishi, K.; Woody, R. W. *Circular Dichroism: Principles and Applications*; Wiley, 2000.

Chapter 3 Synthesis of π -Conjugated Isoxazole Dendrimer Systems

3.1 Introduction

Dendrimers are well-defined, “tree-like” macromolecules, with a high degree of order, due to their well-defined spatial location of functional groups, contributing to their specific function.^{1,2} Dendrimers are particularly interesting because of their unusual chemical and physical properties. As a result, dendrimer materials find applications in a wide range of areas; in organic semiconductors, light harvesting materials,³⁻⁶ catalysis,⁷ targeted drug-delivery^{2,8} and macromolecular carriers.^{9,10}

π -Conjugated dendrimers are very interesting to us because of their potential applications in light harvesting, fluorescent sensors, light emitting diodes and devices based on nonlinear optical interactions.¹¹ A well-known example of a π -conjugated dendritic system is the dendritic polyphenylazomethines (DPA).^{10,12-14} These dendrimers have an electron rich inner layer and an electron poor outer layer. This energy gradient from the core to the periphery makes this dendrimers promising materials for highly efficient organic light emitting diodes. Electron transfer occurs more easily in dendrimers with planar structure than in those with steric hindrance, because π -conjugation is well maintained in a planar structure.³ The initial aim of this project was to synthesize a fully conjugated alternating phenyl-isoxazole dendritic system. This type of dendrimers system has never been reported and we anticipated that the materials would exhibit unique electronic and geometric properties.¹⁵ Literature reports based on aryltriazole analogues closely related to the conjugated alternating phenyl-isoxazole dendrimer systems investigated in this study suggested that these dendrimers possibly exhibit two-photon absorption (TPA) activity.¹⁵ TPA has attracted a vast amount of attention in connection to various applications such as optical data storage, three-dimensional imaging of biological systems, photodynamic therapy, optical power limiting, etc.¹⁵ We also wanted to study the three dimensional packing arrangement of these rigid conjugated dendrons (Figure 3.1). We anticipated that, with increasing generation number, the structure would deviate from a flat structure and adopt a fan-like out of plane structure because of steric constraints.^{3,16}

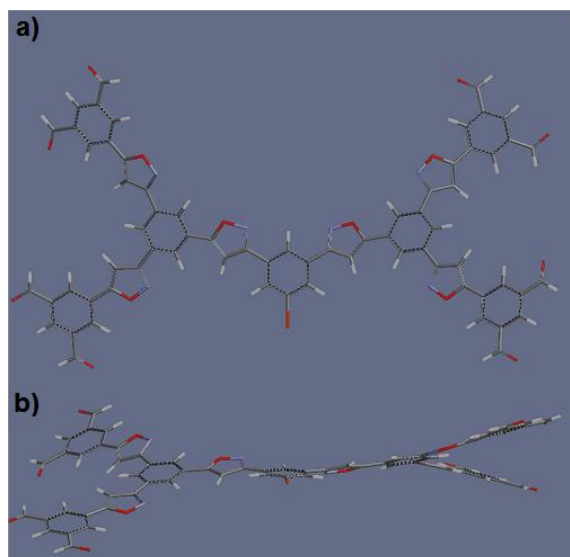


Figure 3.1. Spartan representation of the second generation of a phenyl-isoxazole dendrimer: a) front view showing a supposed flat structure, b) side view showing fan-like out of plane structures.

Dendrimer synthesis

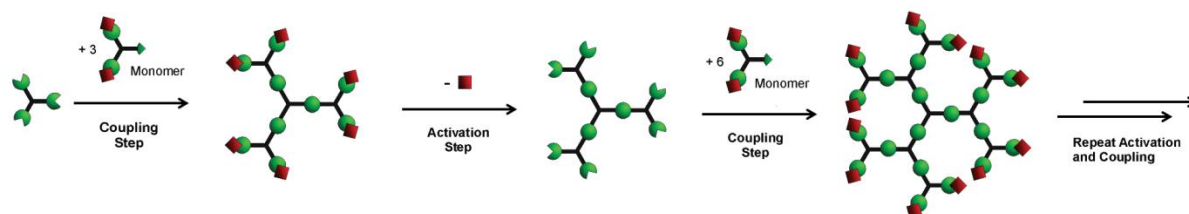
Dendrimers are synthesized by either divergent or convergent pathways (Scheme 3.1).^{2,17-19} The divergent approach commences at the core of the dendrimer and continues to grow outward by repeating successive steps.¹⁸ This growth is initiated by reacting peripheral functionalities of the core with complementary functional groups on the monomer units. The product of the first reaction is called a first generation dendrimer, or G1. Monomer addition introduces a new branching point at coupling sites resulting in next generations (G_n) bearing increased amount of peripheral groups (Scheme 3.3). After completion of the first coupling reaction, the inactivated peripheries can be activated to give new peripheral groups capable of reacting with monomer units.¹⁸ The inactivated functional groups on the monomer units prevent uncontrolled further growth of dendritic generations. Often, after growing each dendritic generation, purification is necessary in order to remove unreacted starting materials and defect dendrimers. The purification is usually performed by column chromatography.²

The convergent approach involves an “inward” growth of the dendrimer system. The construction is induced by activation of the periphery to be coupled to the core molecule. The first reaction results in the first generation dendron also known as the inactivated new periphery of the second generation (G2). This G1 dendron is again activated to be coupled to another core molecule in a 2:1 ratio resulting in the second generation (G2) (Scheme 3.3). It should be noted that the periphery ‘grows’ after each successive step while the same core molecule is used constantly.^{17,18,20} The convergent approach is usually more laborious than the divergent approach, but the

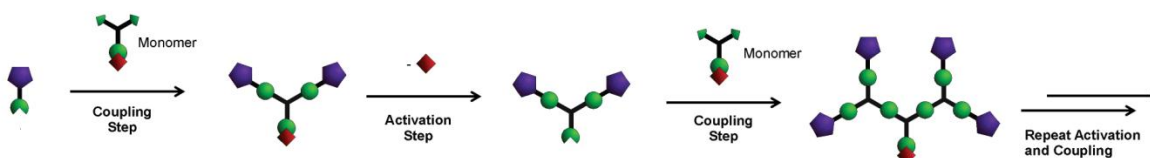
possibility of generating defects in the structure is smaller when using the convergent approach.¹⁷ Both pathways (Scheme 3.3 and Scheme 3.4) were attempted in this study

Scheme 3.1. Schematic representation of divergent and convergent approaches towards dendritic materials.¹⁸

Divergent growth



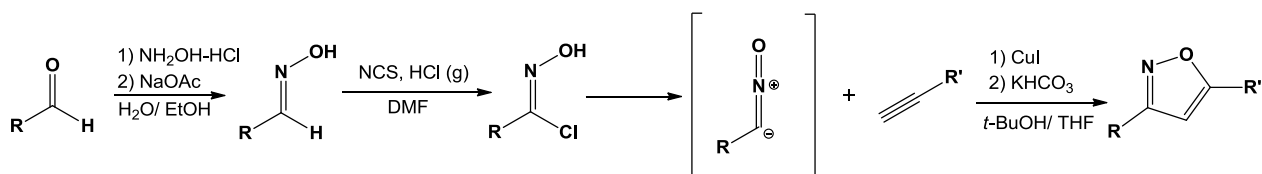
Convergent growth



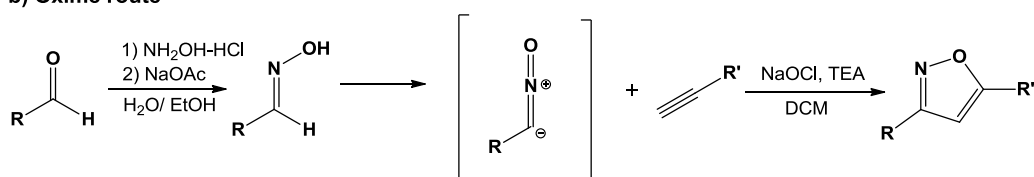
In this study isoxazole moieties were used to link monomer units to the core. Isoxazole formation was indicative of a new generation being formed. Several methods for isoxazole formation have been reported in literature, including approaches based on condensation of 1,3-dicarbonyl compounds with hydroxylamine,²¹ treatment of oxime with *n*-butyllithium in DMF and acid to form an intermolecular cyclization isoxazole,²² and dehydration of 5-hydroxy isoxazoline.²³ In this study we opted to use the Huisgen 1,3-dipolar cycloaddition reaction between nitrile oxides (generated in situ) and terminal alkynes. This was attempted via an imidoyl chloride- and oxime pathway (Scheme 3.2).

Scheme 3.2. Schematic representation of imidoyl chloride²⁴ and oxime routes²⁵ followed.

a) Imidoyl chloride route



b) Oxime route

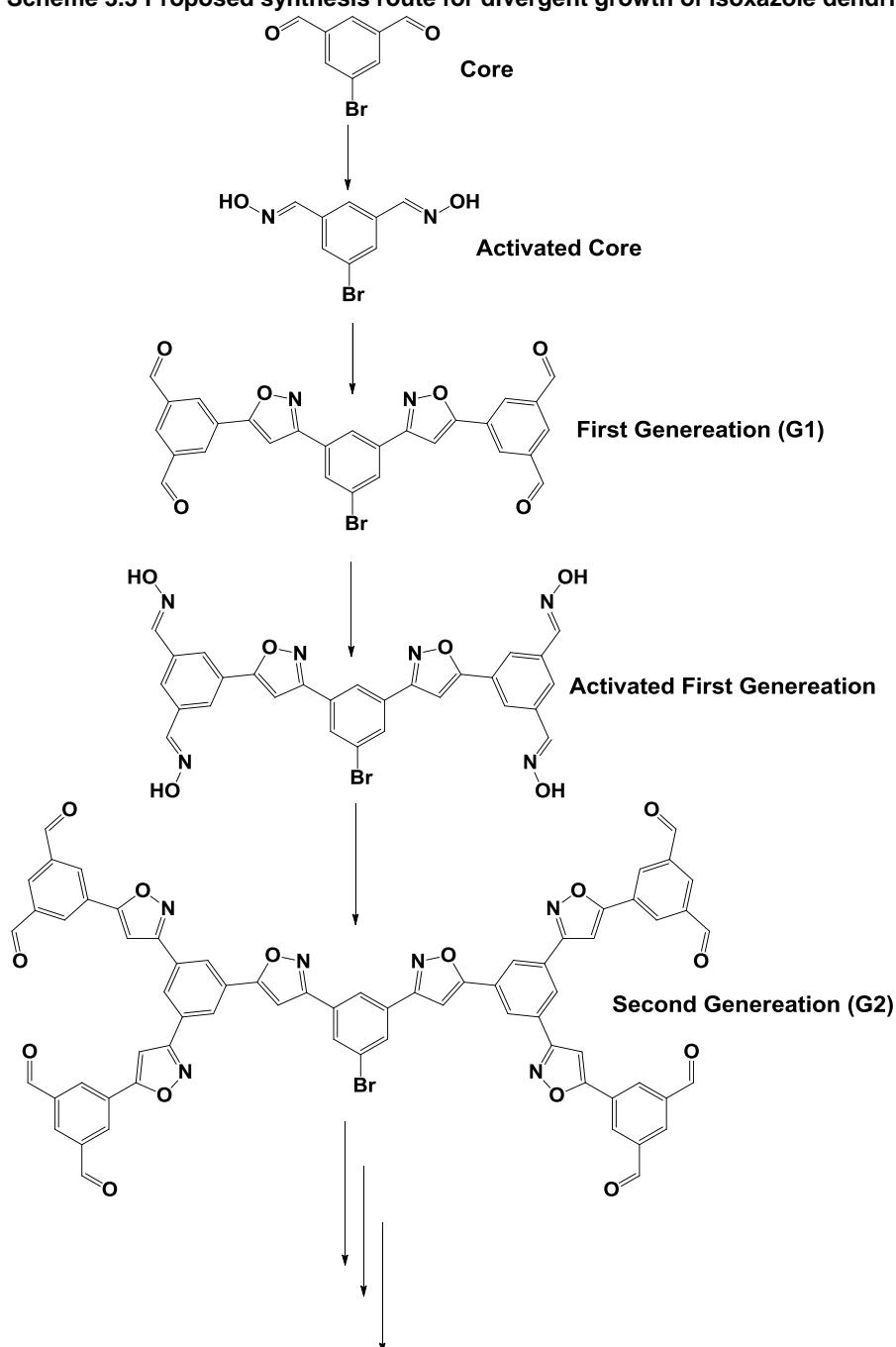


3.2 Our approach

3.2.1 Divergent pathway

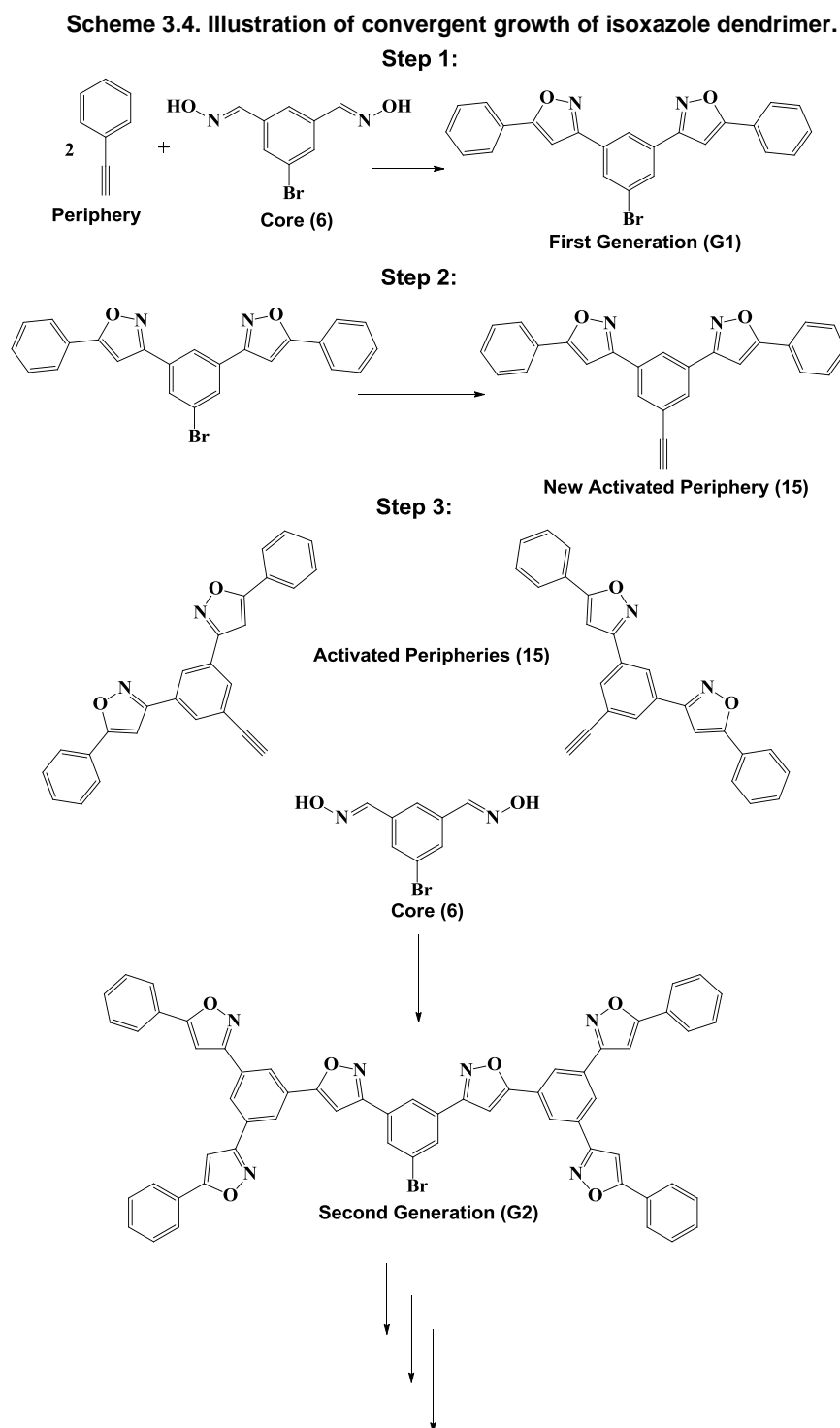
Divergent approach towards conjugated isoxazole dendrimers was attempted by reacting 3,5-dioxime bromobenzene and two terminal alkyne molecules to give a di-isoxazole dendron. By clicking four terminal alkyne molecules to this “first generation” dendron would result in the second generation. By repeating these successive steps, the several generations of the dendrimer can be grown till the sequence becomes limited by solubility. Imidoyl chloride and oxime routes (Scheme 3.2) were attempted in this pathway.

Scheme 3.3 Proposed synthesis route for divergent growth of isoxazole dendrimer.



3.2.2 Convergent pathway

There are three repetitive steps in the route to convergent dendrimer synthesis (Scheme 3.4). In the first step phenyl acetylene is reacted to the core, 3,5 dioxime bromobenzene (**6**), to give generation 1 (G1). Subsequently this newly synthesized G1 dendron is activated by the Sonogashira cross coupling reaction to become the new periphery bearing a terminal alkyne functionality. Finally two of the 'new' periphery molecules, **15**, is reacted with the core, **6**. These three steps are repeated to synthesize higher generations.



3.3 Results and discussion

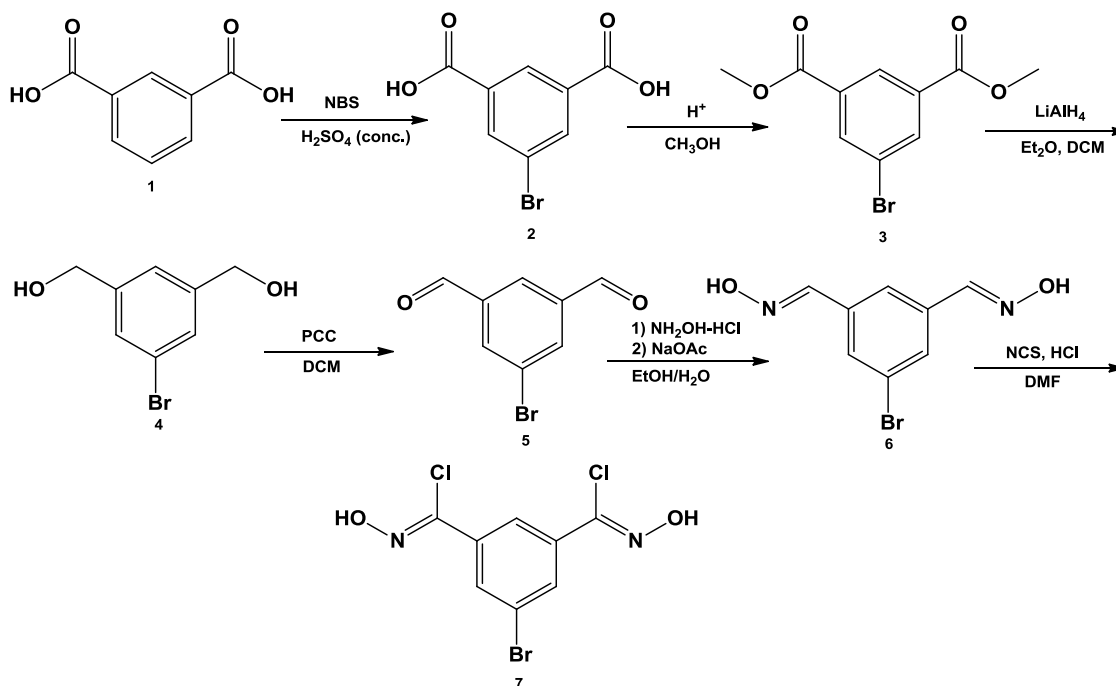
3.3.1 Divergent Pathway

One of the obstacles of this approach was the synthesis of the isoxazole moiety. In this study we opted to use the Huisgen 1,3-dipolar cycloaddition reaction between nitrile oxides (generated *in situ*) and terminal alkynes. In some literature, this has been claimed to be a click reaction.²⁵ This click-reaction was attempted via imidoyl chloride- and oxime pathways.

Imidoyl chloride route

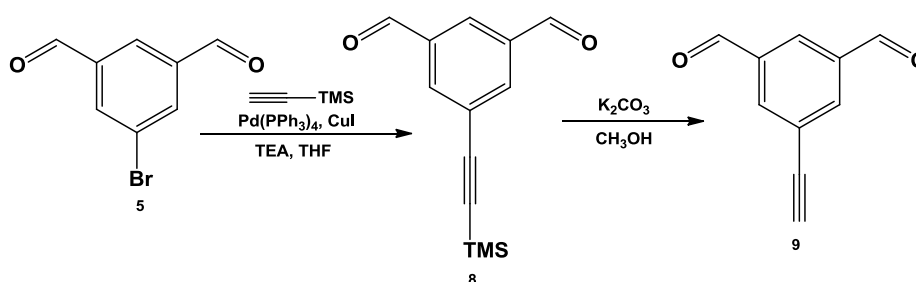
The use of imidoyl chlorides as intermediates in the synthesis of isoxazoles is well documented.²⁶⁻²⁹ Scheme 3.5 shows the proposed strategy for synthesizing the imidoyl chloride core intermediate used in this study. First, isophthalic acid was brominated, using *N*-bromosuccinimide (NBS) in concentrated sulphuric acid, giving 5-bromoisophthalic acid (**2**)³⁰ which was subsequently esterified to give dimethyl-5-bromoisophthalate (**3**) quantitatively.³¹ Reduction of compound **3** then gave 3,5-dimethanol bromobenzene (**4**).³¹ Afterwards, the alcohol groups were selectively oxidized with pyridinium chlorochromate (PCC) to the respective aldehydes forming 5-bromo isophthalaldehyde (**5**).³² Hydroxylamine hydrochloride was then used to transform the two aldehyde functionalities into oxime groups.³³ Finally the dioxime was chlorinated with *N*-chlorosuccinimide (NCS) affording the core intermediate, 5-bromo-*N*-hydroxybenz-di-(1,3)-imidoyl chloride (**7**) in 85% yield.²⁴ The structures were confirmed by mass - , ¹H and ¹³C NMR spectrometry.

Scheme 3.5. Synthesis of the dendrimer core.



The terminal alkyne monomer unit (**9**) was prepared by ethynylating **5** with ethynyltrimethylsilane, via a Sonogashira coupling using, catalyzed by $\text{Pd}(\text{PPh}_3)_4$ and CuI (Scheme 3.6).^{24,34-37} Finally the TMS protecting group was removed, using potassium carbonate, under mild conditions, necessary to preserve the aldehyde functionality, affording **9** in 80% yield.

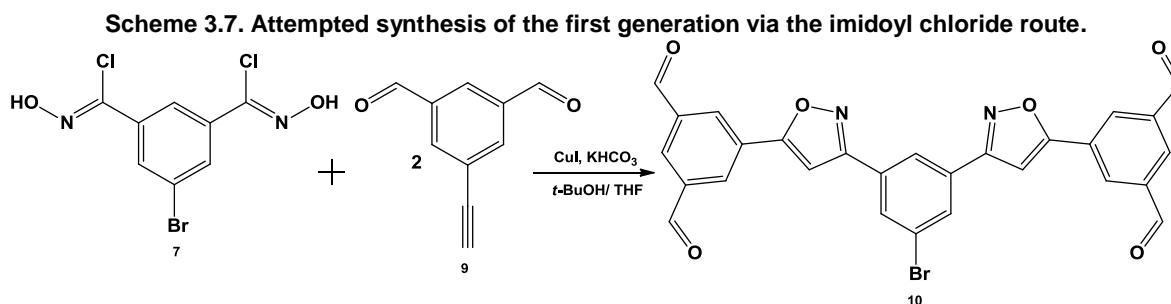
Scheme 3.6 Synthesis of the dendrimer periphery.



The synthesis of the isoxazole moiety was attempted via a [2+3] cycloaddition reaction between the dipolarophile (derived from the alkyne) and the nitrile oxide(s) (generated in situ from imidoyl chlorides - Scheme 3.2). It is known from literature that uncatalyzed 1,3-dipolar cycloadditions reactions between dipolarophiles, derived from activated alkynes, and nitrile oxides generally result in moderate yields and low regioselectivity in the product cycloadduct.²⁴ In a recent study, however, it has been shown Cu catalysis enhances the regioselectivity, forming exclusively the unsymmetrical 3,5-disubstituted isoxazole.^{24,29,38} In this study we used this 'new'

Cu(I) mediated approach in order to realise 3,5-disubstituted isoxazoles with perfect regioselectivity.

We tried to synthesize the bis isoxazole **10** (G1) by “clicking” the di-imidoyl chloride (**7**) with two terminal alkyne units (**9**) (Scheme 3.7) via the Cu(I) catalyzed 1,3-dipolar cycloaddition reaction, however without any success. A possible reason that this reaction was unsuccessful is because of the electronic effects the aldehydes have on the phenyl ring. This will be discussed later in this chapter.



Oxime Route

Vaidya *et al.*²⁵ reported the regioselective synthesis of isoxazoles via 1,3-dipolar cycloaddition. In this approach nitrile oxides are also generated in situ, but from oximes instead of imidoyl chlorides. This approach was adopted to carry out a model study on isoxazole formation using three different benzaldehydes, i.e., benzaldehyde, 4-bromobenzaldehyde and 4-hydroxybenzaldehyde. The aldehyde groups of **11a** and **11b** were first converted to oxime groups, using hydroxylamine hydrochloride (Scheme 3.8), in a facile manner. The conversion to **11c**, however, was not as successful presumably because the nucleophilic character of the hydroxy group on the aromatic ring interfered with oxime formation. Subsequently **11a** and **11b** were treated with sodium hypochlorite and phenyl acetylene to give compounds **12a** and **12b** (Scheme 3.8).

Scheme 3.8. Model study of isoxazole synthesis.

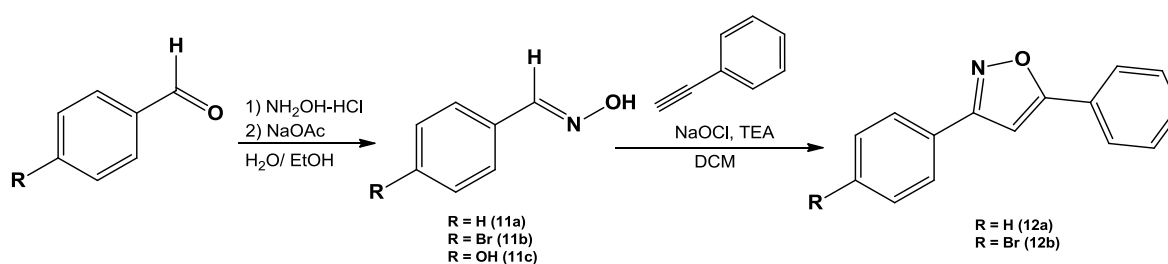


Figure 3.2 shows the comparison of the ^1H NMR spectra of **12a** and **12b** in CDCl_3 . 3,5-Diphenyl isoxazole, **12a**, had only three signals in the aromatic region i.e. a

multiplet from 7.9-7.83 ppm with an integration of 4 corresponding to the 2 protons on each phenyl ring closest to the isoxazole ring (**b** in Figure 3.2i), a multiplet from 7.55-7.42 ppm with an integration of 6 corresponding to 3 protons on each phenyl ring furthest away from the isoxazole ring (**a** in Figure 3.2i), and a singlet at 6.84 ppm with an integration of 1 due to the isoxazole proton. The spectrum of **12b** showed similar peaks to that of **12a** with two extra signals at 7.74 and 7.62 ppm corresponding to the four protons on the aromatic ring with attached bromine. The isoxazole signal was observed at ~6.8 ppm in both spectra. This route proved to be very successful for isoxazole synthesis.

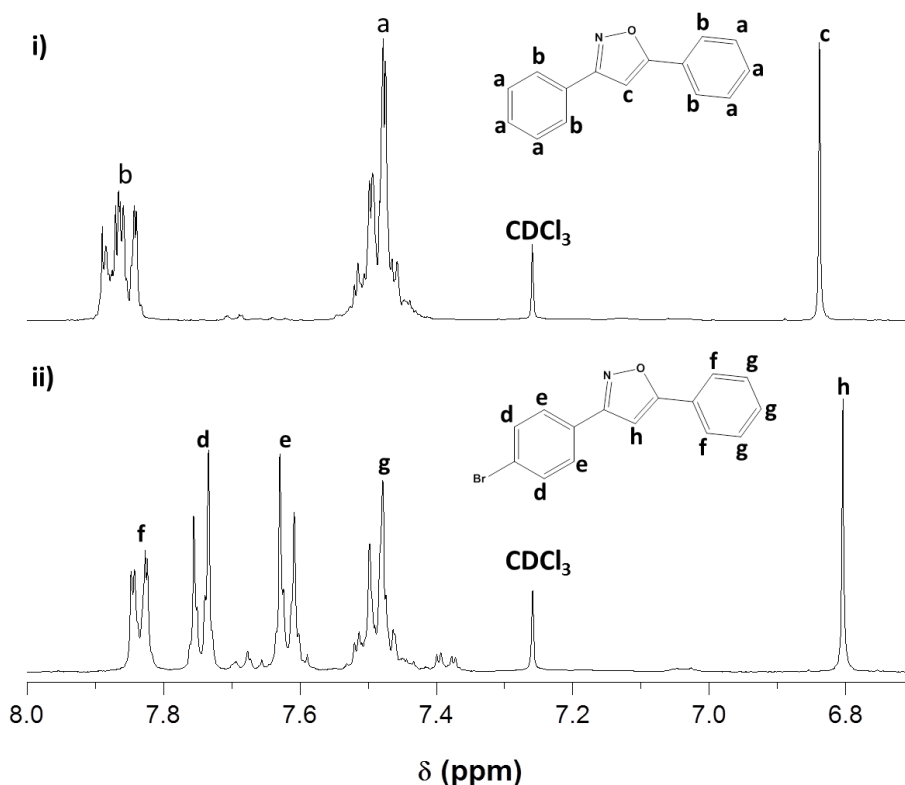
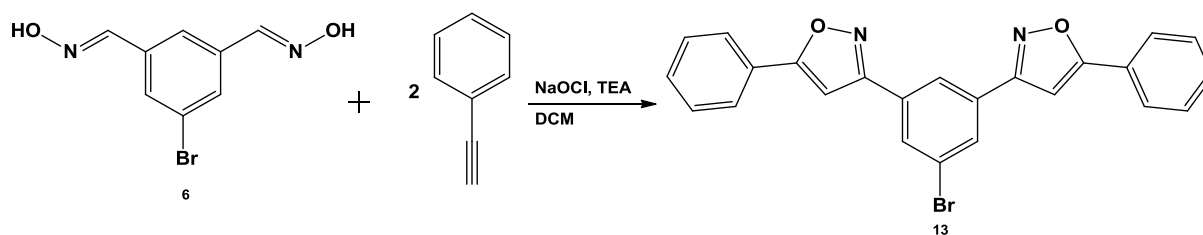


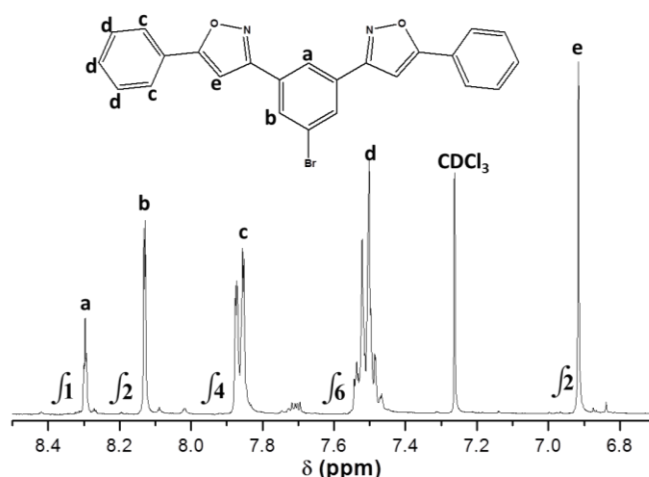
Figure 3.2. i) ^1H NMR spectrum of **12a** and ii) ^1H NMR spectrum of **12b** in chloroform- d_6 between 8.0-6.7 ppm.

After successfully synthesizing the mono-isoxazole functional molecules, we then sought to extend the system to include bis-isoxazole functionality. Using the same procedure as in the model study, 3,5-dioxime bromobenzene (**6**) was treated with phenyl acetylene in the presence of sodium hypochlorite (Scheme 3.9).

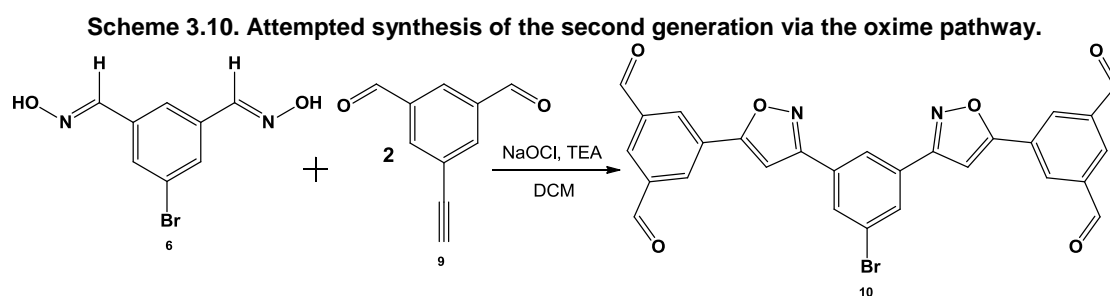
Scheme 3.9. Di-isoxazole synthesis in model study.



The desired product (**13**) was obtained in 30-50% yields. Figure 3.3 shows the ^1H NMR spectrum of the symmetrical 3,5-di-5-phenylisoxazole bromobenzene, **13**. It was clear that the isoxazole was present because of the singlet with integration of two present at 6.9 ppm. The ^{13}C NMR spectrum also showed a characteristic peak for isoxazoles at 97.6 ppm. Mass Spectrometry showed peaks at $m/z = 443$ and 445 showing the molecular ion peak and isotope peak. This investigation confirmed that the di-isoxazole molecule could be successfully synthesized using this procedure.

Figure 3.3. ^1H NMR spectrum of 3,5-di-5-phenylisoxazole bromobenzene (**13**) in CDCl_3 .

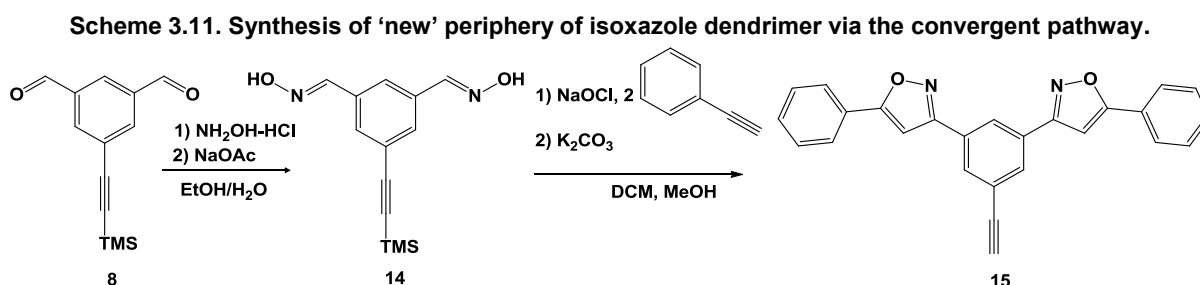
We then proceeded to apply the successful strategy for isoxazole synthesis, into making isoxazole dendrimers via a divergent approach (Scheme 3.9). A successful synthesis (of compound **10**) would then give a molecule with four aldehydes at the periphery which could then be converted/activated into the oxime intermediates necessary for further dendritic growth. The dioxime (**6**) and terminal acetylene (**9**) were reacted, under similar conditions successfully applied for the synthesis of **13**, (Scheme 3.9) however, the synthesis was unsuccessful, and both starting materials were unreacted, even after the temperature was elevated from $25\text{ }^\circ\text{C}$ to $45\text{ }^\circ\text{C}$ and longer reaction times were tried (Scheme 3.10).



A consistent aspect in both failed attempts at dendrimer synthesis (the imidoyl chloride route, Scheme 3.7, and the oxime route, Scheme 3.10) is the presence of aldehyde functionality. We were not able to decipher the role of the aldehyde functionality group in the failure of the experiment within the time frame of the research program. It was speculated that the electron-withdrawing dialdehydes are deactivating the alkyne for the 1,3-dipolar cycloaddition reaction. The alkyne is conjugated with the aromatic ring. Therefore, the electron density in the alkyne will also be decreased with a resulting lower reactivity.

3.3.2 Convergent Pathway

The core, **6**, was prepared by the same facile procedures used in the divergent growth pathway (Scheme 3.5). **13** was prepared by the same procedures used in the model study (Scheme 3.9). Attempts to ethynylate **13** with trimethylsilyl acetylene, via the Sonogashira coupling, failed presumably because the aromatic ring was not sufficiently activated by the isoxazoles groups. To circumvent this, the order in which the reactions were carried out was changed. This procedure gave **15**, the 'new' periphery (Scheme 3.11). Characterization was carried out using ^1H and ^{13}C NMR spectroscopy. The ^1H NMR spectrum of **15** was identical to the ^1H NMR spectrum of **13** (Figure 3.3) except for the extra singlet at 3.21 ppm corresponding to the alkyne proton.



Attempts to react **6** (the core) and **15** were unsuccessful. It was speculated that the steric effects inhibited **15** to come into close proximity to **6**. Synthesis of the first generation of isoxazole dendrimer was successfully carried out. However, synthesis

of the second generation turned out to be unsuccessful. Without synthesis of the second and third generations it would not have been possible to study the packing arrangement and electronic properties of these dendrons.

3.4 Conclusions

Successful synthesis of the isoxazole moiety was achieved by using sodium hypochlorite to couple an oxime and a terminal alkyne. Despite the use of convergent and divergent pathways to synthesize isoxazole dendrimers, it turned out that the synthesis of the second and third generation was not possible under these conditions. In the divergent pathway it was speculated that the origin of the problem lies in the presence of aldehyde groups' electronic property on the aromatic ring. It inhibited the formation of next generations.

3.5 Materials and Methods

3.5.1 Materials

Commercially available reagents and solvents were used without further purification unless stated otherwise. Reactions at room temperature were conducted under ambient laboratory conditions ($T = 18 - 30\text{ }^{\circ}\text{C}$, $p = 720 - 770\text{ mm Hg}$). Sonogashira cross-coupling reactions were performed under an argon atmosphere under standard Schlenk conditions in freshly dry distilled solvents. TLC plates (0.20 mm Silica gel 60, with fluorescent indicator UV254) and Silica gel 60 (0.063 - 0.2 mm/70 - 230 mesh) were purchased from Machery-Nagel. ^1H and ^{13}C NMR spectra were recorded on a Varian VXR 400 MHz instrument and chemical shifts were given in parts per million (ppm) on the delta scale (δ) using solvent peak as a reference value (^1H NMR: $\text{Me}_4\text{Si} = 0.00$, $(\text{CD}_3)_2\text{CO} = 2.05$, $(\text{CD}_3)_2\text{SO} = 2.50$, $\text{CDCl}_3 = 7.27$; ^{13}C NMR: $\text{CDCl}_3 = 77.16$; $(\text{CD}_3)_2\text{CO} = 29.84 + 206.26$, $(\text{CD}_3)_2\text{SO} = 39.52$). Abbreviations for NMR data: s = singlet; br. s. = broad singlet; d = doublet; t = triplet; q = quartet; dd = doublet of doublets; dt = doublet of triples; m = multiplet. Mass spec was performed on a Waters GCT Premier or a Waters API Quattro Micro instrument.

3.5.2 Experimental Procedures

Synthesis of 5-Bromoisophthalic acid (2)

Isophthalic acid (15 g, 90.3 mmol) was dissolved in sulphuric acid (55 mL) and the temperature increased to $60\text{ }^{\circ}\text{C}$. NBS (19.3 g, 108 mmol) was then added to the mixture over a period of 45 minutes and the reaction further stirred for 90 minutes. The reaction was followed by TLC (Ethyl Acetate, 1 % TFA). After consumption of the

starting material, the reaction mixture was poured onto ice (150 g). It was subsequently filtered and washed with H₂O and hexane successively. Recrystallization from a H₂O/acetone mixture (1:4) afforded white crystals in a 95% yield. ¹H NMR (400 MHz, CO(CD₃)₂) δ ppm 4.43 (br. s., 2 H) 8.34 (d, J = 1.56 Hz, 2 H) 8.60 (t, J = 1.56 Hz, 1 H). ¹³C NMR (400 MHz, CO(CD₃)₂) δ ppm 122.99, 130.22, 134.25, 137.08, 165.71.

Synthesis of Dimethyl-5-Bromoisophthalate (3)

5-Bromoisophthalic acid (20 g, 81.6 mmol) was dissolved in methanol (250 mL). A mixture of sulphuric acid (18 mL) to methanol (60 mL) was added after all the starting material has dissolved. The reaction mixture was refluxed for 24 hours. After completion of the reaction it was cooled to ambient temperature before it was placed in an ice bath and cooled to 0 °C. The mixture was filtered and washed with cold methanol. After drying the product a white powder was obtained in 72% yield. ¹H NMR (400 MHz, CDCl₃) δ ppm 3.96 (s, 6 H) 8.36 (d, J =1.56 Hz, 2 H) 8.61 (t, J =1.56 Hz, 1 H) ¹³C NMR (400MHz, CDCl₃) δ ppm 52.66, 122.56, 129.22, 132.29, 136.61, 164.94.

Synthesis of 3,5-Dimethanol bromobenzene (4)

A dry 500 mL three neck flask was filled with dry diethyl ether (~35 mL) and LiAlH₄ (5.06 g) so that all the powder was submerged in the liquid to form a slurry. Dry dimethyl-5-bromoisophthalate (**3**) (14 g, 0.051 mol) was dissolved in dry diethyl ether (100 mL) and DCM (5 mL). This solution (**3**) was added dropwise to the slurry while using an ice bath to cool down the flask. After adding all the starting material to the reaction flask the temperature was increased and the mixture refluxed for 24 hours. After completion of the reaction the mixture was cooled down and ethyl acetate (80 mL) was added slowly. It was then quenched with water (5 mL) and 1M NaOH (5 mL) solution followed by another addition of water (5 mL) and 1 M NaOH (5 mL) while the reaction mixture was submerged in an icebath. The lithium salt that formed was filtered off and washed with more ethyl acetate and diethyl ether. The washings and filtrate was dried with MgSO₄ and the solvent evaporated. A white powder was obtained in 55% yield. ¹H NMR (300 MHz, CO(CD₃)₂) δ ppm 4.39 (t, J = 5.8 Hz, 2H), 4.63 (d, J = 5.8 Hz, 4H), 7.31 (dt, J = 2.2, 1.5, 0.7 Hz, 1H), 7.41 (dd, J = 1.4, 0.7 Hz, 2H). ¹³C NMR (300 MHz, CO(CD₃)₂) δ ppm 63.94, 122.63, 124.17, 128.51, 146.08.

Synthesis of 5-Bromo isophthalaldehyde (5)

3,5-Dimethanol bromobenzene (2 g, 9.21 mmol) **4** and PCC (6.3 g, 29.2 mmol) were taken up into dichloromethane (50 mL). The mixture was refluxed for 20 hours. The reaction mixture was cooled down and the contents were filtered through a silica gel plug and washed with DCM (3 x 50 mL). The solvent was removed and the product was purified by column chromatography (3:1 pentane: ethyl acetate). White powder was obtained in 70% yield. $^1\text{H NMR}$ (400 MHz, CDCl_3) δ ppm 8.25 (d, $J=1.37$ Hz, 2 H) 8.30 (t, $J=1.37$ Hz, 1 H) 10.05 (s, 2 H) $^{13}\text{C NMR}$ (400 MHz, CDCl_3) 124.33, 129.20, 137.14, 138.39, 189.47.

Synthesis of 3,5-Dioxime bromobenzene (6)

5-Bromoisophthalaldehyde **5** (0.5 g, 2.3 mmol) and hydroxylamine hydrochloride (0.652 g, 9.4 mmol) were taken up into a 5:1 ethanol/water mixture (150 mL). The temperature was decreased to 0 °C before sodium acetate (1.15 g, 14 mmol) dissolved in a little water was added. Reaction was stirred at ambient temperature and followed by TLC (3:1 pentane: ethyl acetate). Reaction was stopped after ~3 hours. The ethanol and most of the water was removed under reduced pressure. Water (100 mL) was added to the flask and the product was subsequently extracted with ethyl acetate (2 x 50 mL) and diethyl ether (2 x 50 mL). The organic layers were dried over MgSO_4 . A cream coloured solid was obtained after column chromatography (3:1 pentane: ethyl acetate) (80% yield). $^1\text{H NMR}$ (300 MHz, $\text{CO}(\text{CD}_3)_2$) δ ppm 7.79 (d, $J=1.47$ Hz, 2 H) 7.85 (t, $J=1.25$ Hz, 1 H) 8.16 (s, 2 H) 10.68 (s, 2 H).

Synthesis of 5-Bromo-dihydroxyisophthalimidoyl dichloride (7)

3,5-Dioxime bromobenzene **6** (0.3 g, 1.95 mmol) was dissolved in dimethylformamide (DMF) (60 mL). N-Chlorosuccinimide (NCS) (0.57 g, 4.28 mmol) was added in 5 portions. HCl gas was bubbled through the reaction mixture after each portion was added. After NCS addition, HCl gas was bubbled through the mixture every 2 hours for the first 8 hours of the reaction. Subsequently the reaction was allowed to stir for another 12 hours. After completion, the reaction was diluted with ethyl acetate, washed with water, and dried over MgSO_4 . (85% yield) $^1\text{H NMR}$ (400 MHz, $\text{CO}(\text{CD}_3)_2$) δ ppm 8.06 (d, $J = 1.4$ Hz, 2H), 8.30 (t, $J = 1.5$ Hz, 1H), 11.92 (s, 2H).

Synthesis of 5-(2-(Trimethylsilyl)ethynyl)isophthalaldehyde (8)

5-Bromo isophthalaldehyde **5** (1.5 g, 7 mmol), ethynyltrimethylsilane (1.38 g, 14.1 mmol), triethylamine (10 mL) and tetrahydrofuran (10 mL) was added to a dry Schlenck flask. The solvents were degassed by one freeze-pump-thaw cycle. The flask was opened again to add Pd(PPh₃)₄ (0.16 g, 0.14 mmol) and CuI (26.8 mg, 0.14 mmol). Flask was degassed with three freeze-pump-thaw cycles and filled with argon. Reaction was stirred at 50 °C for 3 hours. After the reaction was finished the salt was filtered off and the solvent removed under reduced pressure. A yellow liquid (70% yield) was obtained after column chromatography (2:1 pentane: DCM). ¹H NMR (400 MHz, CDCl₃) δ ppm 0.29 (s, 9 H) 8.20 (d, $J=1.56$ Hz, 2 H) 8.31 (t, $J=1.56$ Hz, 1 H) 10.08 (s, 2 H) ¹³C NMR (400 MHz, CDCl₃) δ (ppm) -0.30, 98.44, 101.80, 125.69, 129.60, 136.99, 137.62, 190.22.

Synthesis of 5-Ethynyl isophthalaldehyde (9)

5-(2-(Trimethylsilyl)ethynyl)isophthalaldehyde **8** (1.5 g, 6.7 mmol) and K₂CO₃ (0.092 g, 0.67 mmol) were taken up into methanol (100 mL) and stirred under nitrogen atmosphere at ~25 °C. The progress was followed by TLC (4:1 pentane: ethyl acetate). The reaction was stopped after 3 hours and a saturated solution of NaHCO₃ (150 mL) was added and the solution extracted with DCM (4 x 50 mL). The combined extracts were dried with MgSO₄ (anhydrous) and the solvent evaporated. The product was isolated as a cream coloured precipitate (80% yield). ¹H NMR (400 MHz, CDCl₃) δ ppm 3.28 (s, 1 H) 8.23 (d, $J=1.56$ Hz, 2 H) 8.35 (t, $J=1.56$ Hz, 1 H) 10.10 (s, 2 H).

Synthesis of Benzaldehyde oxime (11a)

The same procedure employed for the synthesis of **6** was followed using benzaldehyde as a starting material. After column chromatography (2:1 pentane: ethyl acetate) a yellow oil was obtained in 25% yield. ¹H NMR (300 MHz, CDCl₃) δ ppm 7.35 - 7.46 (m, 3 H) 7.54 - 7.64 (m, 2 H) 7.94 (br. s., 1 H) 8.16 (s, 1 H).

Synthesis of 4-Bromo benzaldehyde oxime (11b)

A procedure employed for the synthesis of **6** was followed using 4-bromobenzaldehyde as a starting material. After column chromatography (3:1 pentane: ethyl acetate) a white powder was obtained in 22% yield. ¹H NMR (400 MHz, CDCl₃) δ ppm 7.44 (td, $J=8.4, 4.1$ Hz, 2 H) 7.52 (td, $J=8.4, 4.1$ Hz, 2 H) 8.06 (s, 1 H) 8.09 (s, 1 H).

Synthesis of 3,5-Diphenyl isoxazole (12a)

Solution of benzaldehyde oxime **6a** (0.2 g, 1 mmol), phenylacetylene (0.11 mL), 3 drops of TEA, and dichloromethane (10 mL) were cooled to 0 °C. To this solution, 10-15% NaOCl (3.33 mL in 6.66 mL H₂O) was added dropwise stirring at 0 °C. The reaction mixture was warmed to room temperature for 10 hours. After consumption of the oxime (TLC 1:1 pentane: DCM) the reaction phases were separated and the aqueous phase was extracted with dichloromethane. The combined organic phases were washed with brine and dried over MgSO₄. The crude product obtained was purified by column chromatography (5:1 Pentane:DCM). Off-white crystals was obtained in 54% yield. ¹H NMR (400 MHz, CDCl₃) δ ppm 6.85 (s, 1 H) 7.43 - 7.56 (m, 6 H) 7.83 - 7.92 (m, 4 H).

Synthesis of 3-(4-Bromophenyl)-5-phenylisoxazole (12b)

A similar procedure used for making 3,5-diphenyl isoxazole **12a** was used to make **12b**. A yellow solid (71%) was obtained after column chromatography (2:1 pentane: DCM). ¹H NMR (400 MHz, CDCl₃) δ ppm 6.81 (s, 1 H) 7.46 - 7.53 (m, 3 H) 7.60 - 7.65 (m, 2 H) 7.73 - 7.78 (m, 2 H) 7.82 - 7.87 (m, 2 H) ¹³C NMR (400 MHz, CDCl₃) δ ppm 97.48, 124.54, 126.07, 127.50, 128.31, 128.54, 129.27, 130.60, 132.39, 162.29, 170.98.

Synthesis of 3,5-di-5-phenylisoxazole bromobenzene (13)

A similar procedure used for synthesizing **12a** and **12b** was used to synthesize **13**. 3,5-dioxime bromobenzene (**6**) was used as the starting material together with 2 equivalents of phenylacetylene. The crude product was purified by column chromatography (1:1 pentane: DCM) and a cream coloured solid was obtained in 25% yield. ¹H NMR (400 MHz, CDCl₃) δ ppm 6.92 (s, 2 H) 7.49 - 7.56 (m, 6 H) 7.87 (dd, $J=8.01, 1.76$ Hz, 4 H) 8.14 (d, $J=1.56$ Hz, 2 H) 8.30 (t, $J=1.46$ Hz, 1 H) ¹³C NMR (400 MHz, CDCl₃) δ ppm 97.40, 123.59, 123.74, 125.89, 127.12, 129.10, 130.52, 131.00, 131.72, 161.31, 171.11.

Synthesis of 3,5-Dioxime (trimethylsilyl)ethynyl-benzene (14)

5-(2-(Trimethylsilyl)ethynyl)isophthalaldehyde **8** (0.12 g, 0.76 mmol) and hydroxylamine hydrochloride (0.22 g, 3.19 mmol) were taken up into a 5:1 ethanol/water mixture (30 mL). The temperature was decreased to 0 °C before sodium acetate dissolved in a little water (0.39 g, 4.78 mmol) was added. Reaction was stirred at ambient temperature and followed by TLC (3:1 pentane: ethyl acetate). Reaction was stopped after ~3 hours. The ethanol and most of the water was

removed under reduced pressure. Water (100 mL) was added and product was extracted with ethyl acetate (2 x 50 mL) and diethyl ether (2 x 50 mL). The organic layers were dried over MgSO_4 . A white solid was obtained after column chromatography (2:1 pentane: ethyl acetate) (27% yield). $^1\text{H NMR}$ (300 MHz, $\text{CO}(\text{CD}_3)_2$) δ ppm 0.24 (s, 9H), 7.68 (d, $J = 1.3$ Hz, 2H), 7.90 (t, $J = 1.3$ Hz, 1H), 8.17 (s, 2H), 10.62 (s, 2H). $^{13}\text{C NMR}$ (400 MHz, $\text{CO}(\text{CD}_3)_2$) δ ppm -0.12, 95.55, 104.73, 124.74, 125.26, 131.04, 135.20, 148.20.

Synthesis of 3,3'-(5-Ethynyl-1,3-phenylene)bis(5-phenylisoxazole) (15)

3,5 Dioxime (trimethylsilyl)ethynyl-benzene **14** (0.5 g, 1.9 mmol), phenyl acetylene (0.633 mL, 5.8 mmol), and 3 drops of TEA were added to dichloromethane (10 mL) containing 3 drops of acetone to solvate the starting materials. The reaction mixture was cooled to 0 °C. To this solution, 10-15% NaOCl (3 mL in 6 mL H_2O) was added dropwise while stirring at 0 °C. The reaction mixture was warmed to room temperature for 10 hours. After consumption of the oxime the reaction phases were separated and the aqueous phase was extracted with DCM. The combined organic phases were washed with brine and dried over MgSO_4 . The crude product obtained was purified by column chromatography (9:1 pentane: Et_2O). The TMS protected product (0.48 g, 1.04 mmol) was taken up into 5 mL DCM. To this solution tetra-*n*-butylammonium fluoride (TBAF) (0.545 g, 2.1 mmol) was added and the reaction mixture was stirred for 5 minutes. Column Chromatography (9:1 pentane: Et_2O) afforded the product in 8% yield. $^1\text{H NMR}$ (300 MHz, CDCl_3) δ 3.20 (s, 1H), 6.90 (s, 2H), 7.55 – 7.45 (m, 6H), 7.89 – 7.81 (m, 4H), 8.07 (d, $J = 1.6$ Hz, 2H), 8.34 (t, $J = 1.6$ Hz, 1H). $^{13}\text{C NMR}$ (400 MHz, CDCl_3) δ ppm 97.57, 123.99, 125.41, 126.02, 127.00, 127.34, 129.23, 130.44, 130.60, 131.72, 161.85, 171.13.

3.5 References

- (1) Balzani, V.; Ceroni, P.; Maestri, M.; Vicinelli, V. *Current Opinion in Chemical Biology* **2003**, 657.
- (2) Carlmark, A.; Hawker, C.; Hulta, A.; Malkoch, M. *Chem. Soc. Rev.* **2009**, 38, 352.
- (3) Kodama, Y.; Ishii, S.; Ohno, K. *J. Phys.: Condens. Matter* **2009**, 21, 1.
- (4) Akai, I.; Miyanari, K.; Shimamoto, T.; Fujii, A.; Nakao, H.; Okada, A.; Kanemoto, K.; Karasawa, T.; Ishida, A.; Yamada, A.; Katayama, I.; Takeda, J.; Kimura, M. *Physica Status Solidi C Current Topics in Solid State Physics* **2009**, 6, 77.
- (5) Kodama, Y.; Ishii, S.; Ohno, K. *J. Phys.: Condens. Matter* **2007**, 19, 1.
- (6) Nantalaksakul, A.; Reddy, D. R.; Bardeen, C. J.; Thayumanavan, S. *Photosynth. Res.* **2006**, 87, 133.
- (7) Ornelas, C.; Aranzaes, J. R.; Salmon, L.; Astruc, D. *Chem. Eur. J.* **2008**, 14, 50.
- (8) Menjoge, A. R.; Kannan, R. M.; Tomalia, D. A. *Drug Discovery Today* **2010**, 15, 171.
- (9) Hecht, S.; Fréchet, J. M. J. *Angew. Chem., Int. Ed.* **2001**, 40, 74.
- (10) Higuchi, M.; Tsuruta, M.; Chiba, H.; Shiki, S.; Yamamoto, K. *J. Am. Chem. Soc.* **2003**, 125, 9988.
- (11) Melinger, J. S.; Davis, B. L.; McMorrow, D.; Pan, Y.; Peng, Z. *J. Fluoresc.* **2004**, 14, 105.
- (12) Higuchi, M.; Shiki, S.; Yamamoto, K. *Org. Lett.* **2000**, 2, 3079.
- (13) Nakajima, R.; Tsuruta, M.; Higuchi, M.; Yamamoto, K. *J. Am. Chem. Soc.* **2004**, 126, 1630.
- (14) Higuchi, M.; Shiki, S.; Ariga, K.; Yamamoto, K. *J. Am. Chem. Soc.* **2001**, 123, 4414.
- (15) Parent, M.; Mongin, O.; Kamada, K.; Katana, C.; Blanchard-Desce, M. *Chem. Commun. (Cambridge, U. K.)* **2005**, 2029.
- (16) Albrecht, K.; Yamamoto, K. *J. Am. Chem. Soc.* **2009**, 131, 2244.
- (17) Simanek, E. E.; Gonzalez, S. O. *J. Chem. Educ.* **2002**, 79, 1222.
- (18) Grayson, S. M.; Fréchet, J. M. J. *Chem. Rev. (Washington, DC, U. S.)* **2001**, 101, 3819.
- (19) Tomalia, D. A.; Baker, H.; Dewald, J.; Hall, M.; Kallos, G.; Martin, S.; Roeck, J.; Ryder, J.; Smith, P. *Polym. J. (Tokyo, Jpn.)* **1985**, 17, 117.
- (20) Hawker, C. J.; Fréchet, J. M. J. *J. Am. Chem. Soc.* **1990**, 112, 7638.
- (21) David H. Brown; Styring, P. *Liq. Cryst.* **2003**, 30, 23.
- (22) Gary N. Barber; Olofson, R. A. *J. Org. Chem.* **1978**, 43, 3015.
- (23) V. G. Nenajdenko; S. V. Pronin; Balenkova, E. S. *Russian Chemical Bulletin, International Edition* **2007**, 56, 336–344.
- (24) Vieira, A. A.; Bryk, F. R.; Conte, G.; Bortoluzzi, A. J.; Gallardo, H. *Tetrahedron Lett.* **2009**, 50, 905.
- (25) Vaidya, V. V.; Wankhede, K. S.; Salunkhe, M. M.; Trivedi, G. K. *Can. J. Chem.* **2008**, 86, 138.
- (26) Goyard, D.; Telligmann, S. M.; Goux-Henry, C.; Boysen, M. M. K.; Framery, E.; Gueyrard, D.; Vidal, S. *Tetrahedron Lett.* **2010**, 51, 374.
- (27) Nunno, L. D.; Vitale, P.; Scilimati, A. *Tetrahedron* **2008**, 64, 11198.
- (28) Vieira, A. A.; Bryk, F. R.; Conte, G.; Bortoluzzi, A. J.; Gallardo, H. *Tetrahedron Lett.* **2009**, 50.
- (29) Himo, F.; Lovell, T.; Hilgraf, R.; Rostovtsev, V. V.; Noodleman, L.; Sharpless, K. B.; Fokin, V. V. *J. Am. Chem. Soc.* **2005**, 127, 210.
- (30) Rajesh, K.; Somasundaram, M.; Saiganesh, R.; Balasubramanian, K. K. *J. Org. Chem.* **2007**, 72, 5867.
- (31) Sherrod, S. A.; Costa, R. L. d.; Barnes, R. A.; Boekelheide, V. *J. Am. Chem. Soc.* **1974**, 96, 1565.

- (32) Westcott, N. P.; Pulsipher, A.; Lamb, B. M.; Yousaf, M. N. *Langmuir* **2008**, *24*, 9237.
- (33) Quan, C.; Kurth, M. *J. Org. Chem.* **2004**, *69*, 1470.
- (34) Wang, C.; Batsanov, A. S.; Bryce, M. R. *J. Org. Chem.* **2006**, *71*, 108.
- (35) Tougeri, A.; Negri, S.; Jutand, A. *Chem. Eur. J.* **2007**, *13*, 666.
- (36) Doucet, H.; Hierso, J.-C. *Angew. Chem., Int. Ed.* **2007**, *46*, 834
- (37) Chinchilla, R.; Najera, C. *Chem. Rev. (Washington, DC, U. S.)* **2006**, *107*, 874.
- (38) Iwakura, Y.; Uno, K.; Hong, S.-J.; Hongo, T. *Polym. J. (Tokyo, Jpn.)* **1971**, *2*, 36.

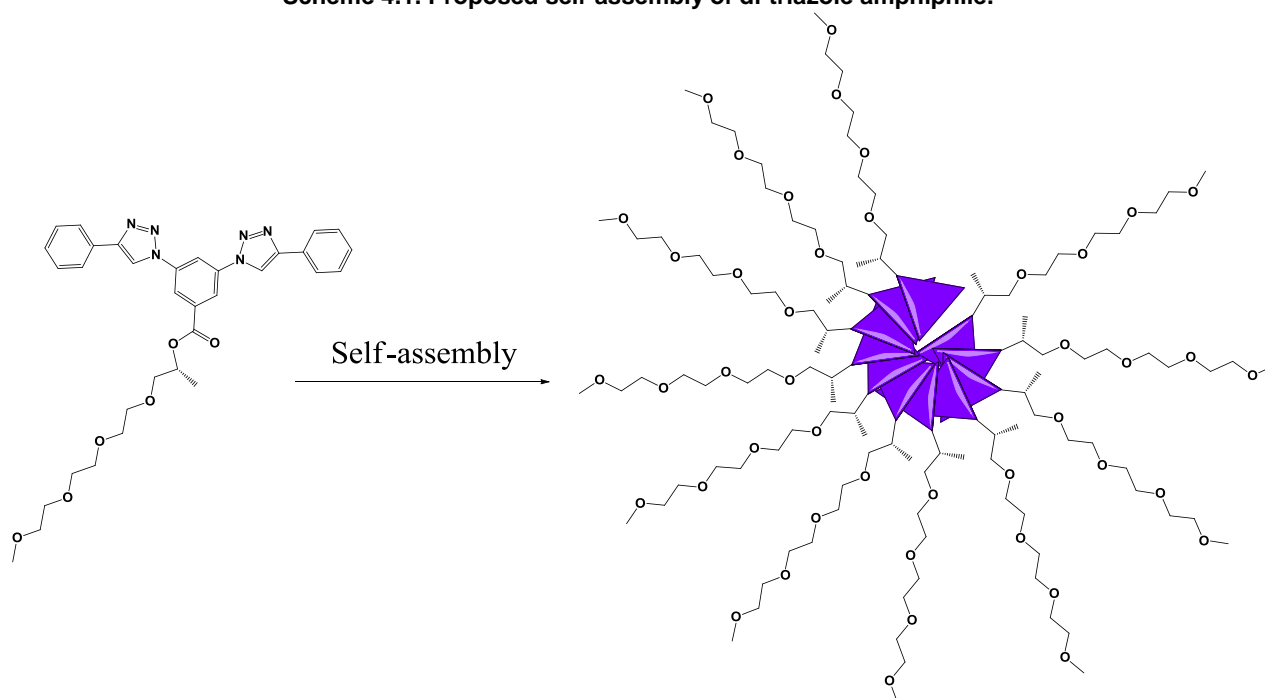
Chapter 4 Triazole Amphiphilic Materials

4.1 Introduction

The helix is an interesting motif and is one of the most frequently occurring secondary structural motifs used in nature.¹⁻⁶ It is not surprising, therefore, that the synthesis of artificial helical structures has fascinated a large number of scientists.⁷⁻¹¹ One interesting example of this phenomenon is provided by amphiphilic discotic molecules, which stack and form helices.^{12,13} The helical structures are stabilized by non-covalent interactions like π - π interactions and van der Waals interactions.

We sought to investigate the ability of amphiphilic molecules based on a conjugated phenyl triazole discotic core tethered with polar side chains to self-assemble into helical supramolecules (Scheme 4.1). These types of molecules are known to be planar,¹⁴ therefore we anticipated that they have the potential to stack and self-organize into higher order structures, stabilized by π - π interactions.^{12,15,16} The self-assembly of these amphiphilic materials posed to be an interesting topic to explore because phenyl triazole discotic amphiphilic materials are not well documented and also because their relatively facile synthetic procedures, *i.e.* the copper-catalysed azide-alkyne cycloaddition.¹⁷⁻²²

Scheme 4.1. Proposed self-assembly of di-triazole amphiphile.



Self-assembly of amphiphilic discotic molecules into helical structures is driven by solvophobicity.^{23,24} In a “good solvent”, both the discotic conjugated core and the side

chains are effectively solvated. When a polar (“poor”) solvent, which selectively solvates the side chains better, is added, the hydrophobic conjugated cores aggregate, in order to minimize interactions with the unfavorable solvent.²⁵ The polar side chains are directed towards the solvent keeping the aggregates solvated, depending on concentration and/or temperature.²⁶ Examples of aprotic (good) solvents for self-assembly of discotic molecules include dimethylformamide (DMF), dimethylsulfoxide (DMSO), and acetonitrile. Good solvents applicable to this study include DMF and acetonitrile because it solvated the whole molecule while water was used as the poor solvent because of the hydrophobicity of the conjugated core and selective solvation of the polar side chains.

Discotic amphiphiles can self-assemble to form left or right handed helices. We appended the conjugated phenyl triazole core with enantiopure chiral oligo(ethylene glycol) side chains in order to bias the twist sense of the formed helices. Enantiomerically pure discotic amphiphiles have previously been used to drive the stacking into single-handed helices.^{15,27,28}

We anticipated that these new triazole amphiphilic molecules would spontaneously aggregate into helices, driven by solvophobic forces. Two amphiphilic molecules were synthesized in this study. The first one carried one chiral side chain attached to the phenyl triazole discotic core (mono side chain amphiphile) and the second one has three chiral side chains attached to the core (tri side chain amphiphile).

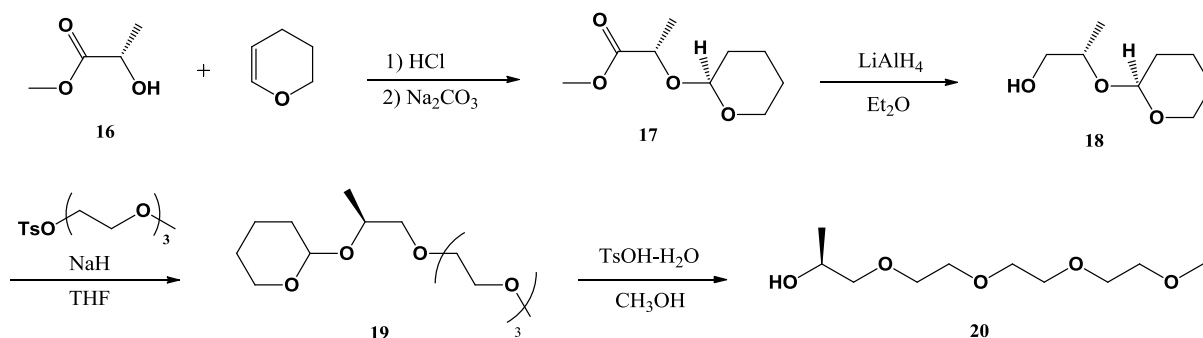
4.2 Results and discussion

4.2.1 Mono side chain amphiphile

Mono side chain amphiphilic molecules were synthesized by incorporating a chiral tetraethylene glycol derivative onto 3,5-diazidobenzoic acid before phenyl acetylene was clicked to the di-azide product resulting in the di-triazole amphiphile.

4.2.1.1 Chiral side chain synthesis

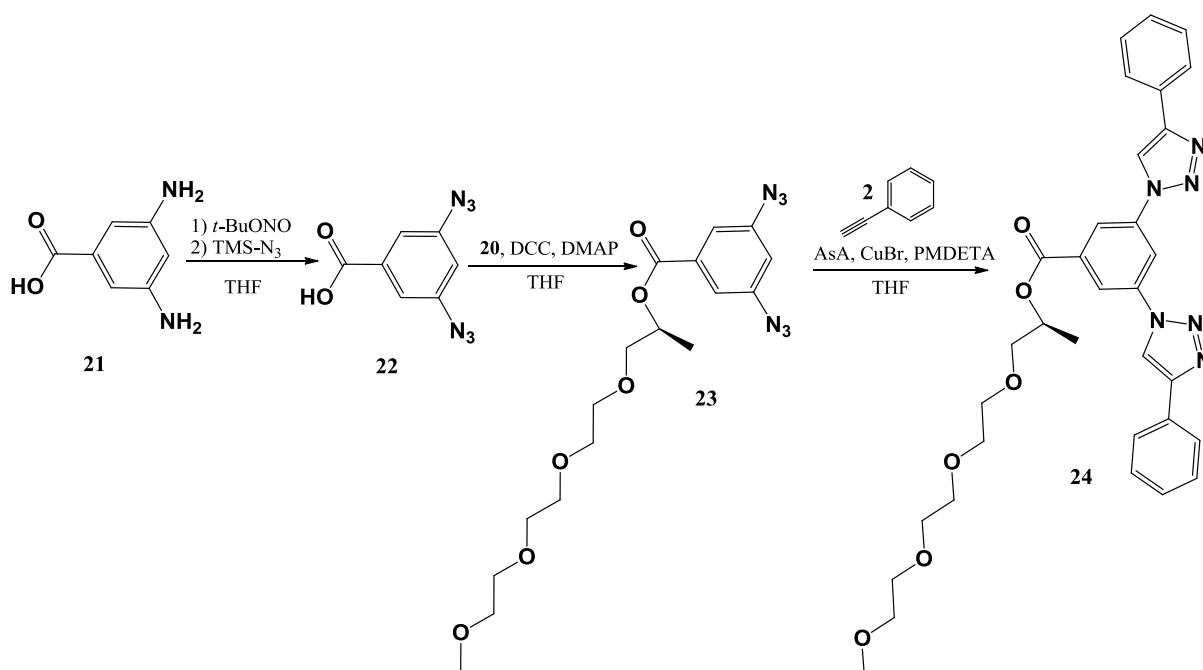
The polar chiral side chain was synthesized by protecting the hydroxyl group of methyl (S)-lactate, **16**, with 2,3-dihydro-2H-pyran to give the chiral protected ether, **17**, (Scheme 4.2). The protected product was subsequently reduced to the primary alcohol, **18**, before it was treated with tosylated triethylene glycol to give, **19**. Lastly the tetrahydropyrane protecting group was removed to give the chiral side chain, **20**.

Scheme 4.2. Synthesis of chiral side chain.²⁹

4.2.1.2 Mono side chain amphiphile synthesis

The mono side chain amphiphile was synthesized by first treating 3,5-diaminobenzoic acid, **21**, with *tert*-butyl nitrite and trimethylsilyl azide to give 3,5-diazidobenzoic acid, **22**, before esterifying **22** with **20** to obtain compound **23**. Finally **23** was clicked with phenyl acetylene, via the copper catalyzed azide-alkyne cycloaddition reaction (Scheme 4.3).

Scheme 4.3. Synthesis of amphiphile bearing one side chain.



Successful characterization of this amphiphilic molecule was followed by investigation of the self-assembly behavior. Self-assembly studies were conducted with UV-vis and CD spectrometry as analytical tools.

4.2.1.3 Analysis of aggregation behaviour

UV-vis

The UV-vis spectra of self-assembled aggregates, in solution, are often characterized by significant red shifts compared to the unimolecularly-dissolved discotics. This is usually considered as evidence for the formation of aggregates.^{16,30-32} Another important characteristic of aggregation is the hypochromicity observed in the UV-vis spectra of molecules. This is a very important feature indicating the formation of an ordered secondary structure. Other important variables, added to solvent quality, which can influence aggregation behavior, are concentration and temperature. Often aggregation is induced by increasing concentration or by lowering temperature.

First we carried out a solvent dependent study in order to determine at what solvent composition **24** shows signs of aggregation (Figure 4.1a) Subsequently, an experiment was set up to show the effects of the concentration of **24** (Figure 4.1b). The solvent dependent studies were done as a trial to show at what solvent composition aggregation is taking place (Figure 4.1a). The samples were analyzed in a DMF/ H₂O solvent system ranging from 100:0 DMF/ H₂O to 10:90 DMF/ H₂O while the concentration was kept constant at 0.27 mM (Figure 4.1b). A hypochromic effect was observed with increased water content. This hypochromicity proved that aggregation was taking place when the H₂O fraction was increased from 0% H₂O to 80% H₂O.

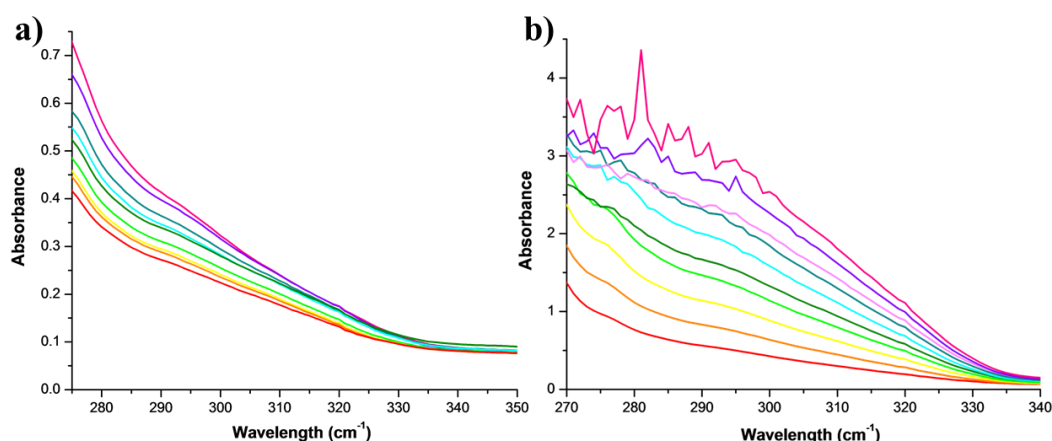


Figure 4.1. UV-vis spectra of 24: (a) solvent dependent experiments varying the solvent from 100:0 DMF/ H₂O to 10:80 DMF/ H₂O (violet = lowest H₂O%, red = high H₂O%, (b) concentration dependent studies carried out in a 90:10 DMF/ H₂O solution. (red = lowest concentration 0.00272 mM; violet = highest concentration 0.272 mM).

Turbidity was observed beyond 80% H₂O content. The material precipitated from the solution after aggregation was observed. Hence, solubility reduces the window of solvent composition between molecularly dissolved samples and samples where aggregates are formed.

Concentration dependent studies were carried out on samples with concentration ranging from 0.0027 mM to 0.27 mM dissolved in a 90:10 DMF/ H₂O solution. From 0.245 mM, the solutions were visibly turbid causing the absorptions to deviate from the trend set by the lower concentrations. Concentration dependent studies showed an increase in absorption with increase in concentration, but showed no conclusive evidence of aggregation taking place.

Circular dichroism

Circular dichroism (CD) is a very powerful technique for studying secondary structures. The formation of a biased helical aggregate can be shown by CD-spectroscopy. Thus CD can prove that a one handed helical structure has formed. If both left and right handed helices are present in a racemic mixture, the CD will show no activity.

In the first experiment, acetonitrile/ H₂O solvent compositions were varied from 0%-90% H₂O composition. The CD spectrum obtained is given in Figure 4.2a. A weak Cotton effect was observed, which proves helix formation. It is important to note that as expected, the observed Cotton effect increased with increased water content.

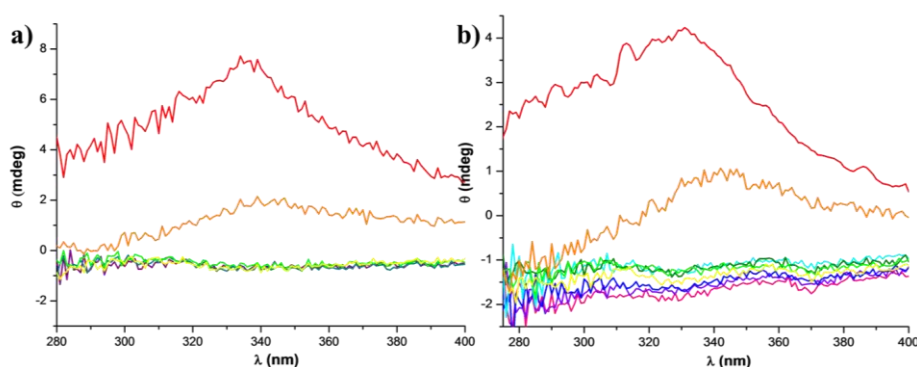


Figure 4.2. CD spectra of 24 (a) 100:0 acetonitrile/ H₂O to 10:90 acetonitrile/ H₂O (red line = 10:90 acetonitrile/ H₂O; orange line = 20:80 acetonitrile/ H₂O; other colours = 40:60 acetonitrile/ H₂O to 100:0 acetonitrile/ H₂O), (b) 10-90% H₂O solution in a mother solution of 10:90 DMF/ acetonitrile (red line = 90% H₂O; orange line = 80% H₂O and the rest of the colours is from 70-10% H₂O).

In a second experiment a 90:10 acetonitrile: DMF mother solution was used to prepare samples containing 10% to 90% H₂O. Figure 4.2b shows the CD spectrum of these samples. A weak Cotton effect was observed in the samples with the highest water content. Helix formation is enhanced by the addition of water.

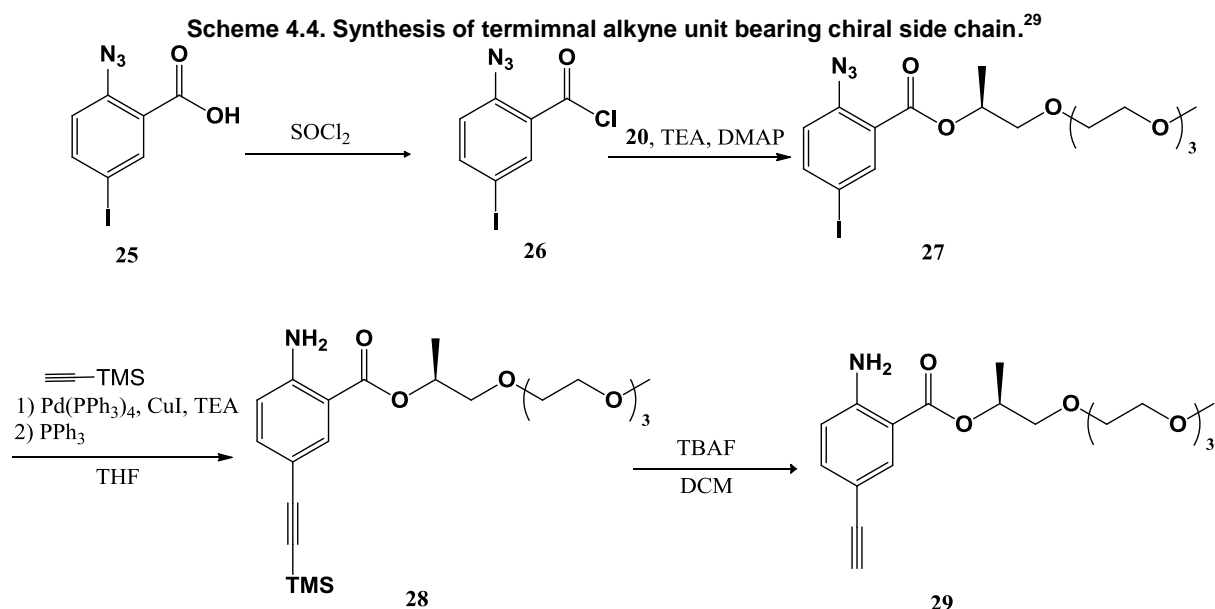
Solubility posed to be the biggest obstacle in the self-assembly of **24**. Therefore, introduction of more polar side chains would enhance the solubility of these molecules in polar solvents (in this case H₂O). A strategy was developed to introduce two more chiral side chains to the system resulting in discotic molecules bearing three chiral side chains (tri side chain amphiphile).

4.2.2 Tri side chain amphiphile

Synthesis of the amphiphile bearing three chiral side chains was carried out by using the same procedure as the amphiphile bearing one chiral side chain. Derivatized phenyl acetylene bearing one chiral side chain on the *meta* position to the alkyne was used instead of phenyl acetylene. The chiral polar side chain was introduced to enhance the solubility and to give the resulting discotic amphiphilic molecule increased chiral information. Chirality is known to drive helical self-assembly.

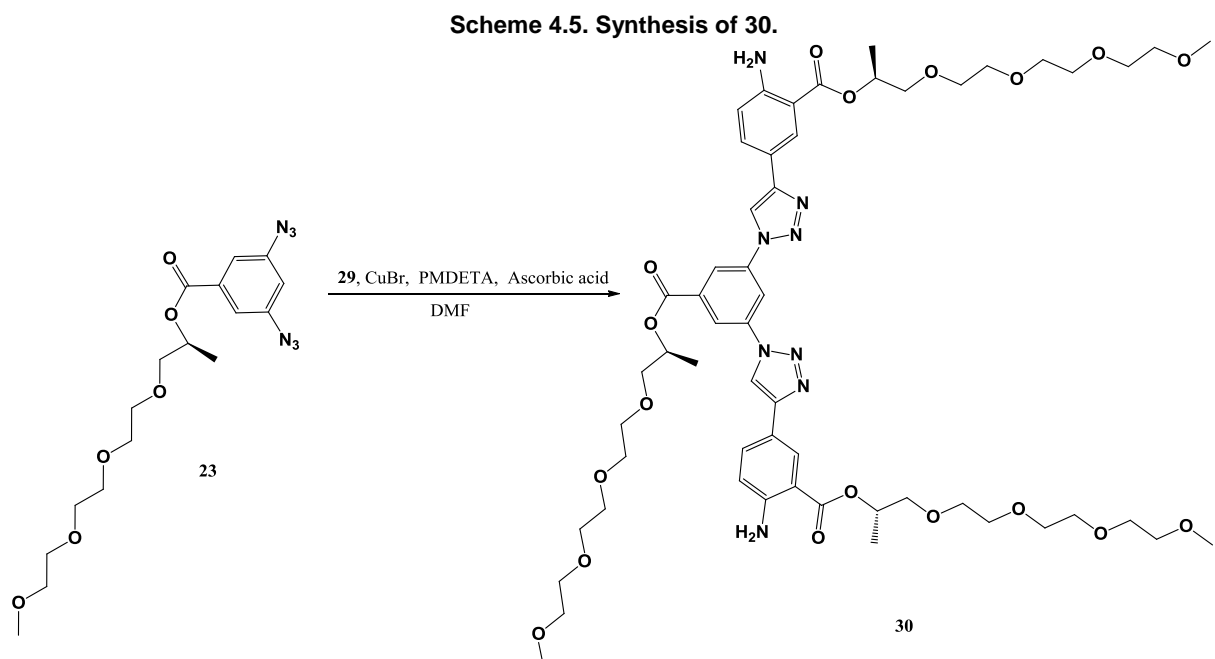
4.2.2.1 Chiral terminal alkyne synthesis

First 2-azido-5-iodobenzoic acid, **25**, was converted to the acid chloride, **26**, before it was treated with (S)-2,5,8,11-tetraoxatetradecan-13-ol, **20**. The resulting product, **27**, was subsequently coupled to ethynyl trimethylsilyl via a Sonogashira coupling, giving **28**. Finally the trimethylsilyl protecting group was removed using tetra-*n*-butylammonium fluoride (TBAF) resulting in **29** (Scheme 4.4).



4.2.2.2 Tri side chain amphiphile synthesis

The amphiphilic molecule, **30**, was synthesized using the same procedure used for synthesis of **24**. The di-azide chiral molecule, **23**, was clicked to **29** via the copper catalyzed azide alkyne cycloaddition reaction to give the desired product, **30**, in 64% yield (Scheme 4.5).



Tri side chain amphiphile, **30**, was characterized by mass spectrometry and ^1H and ^{13}C NMR spectrometry. The symmetry of the molecule made the assignment of all 74 protons less tedious. Figure 4.3 shows the ^1H NMR spectrum of **30** in CDCl_3 . Electron spray ionization mass spectrometry (ES⁺) showed a well-defined molecular ion peak at m/z 1139.55 convincingly proving the formation of this molecule.

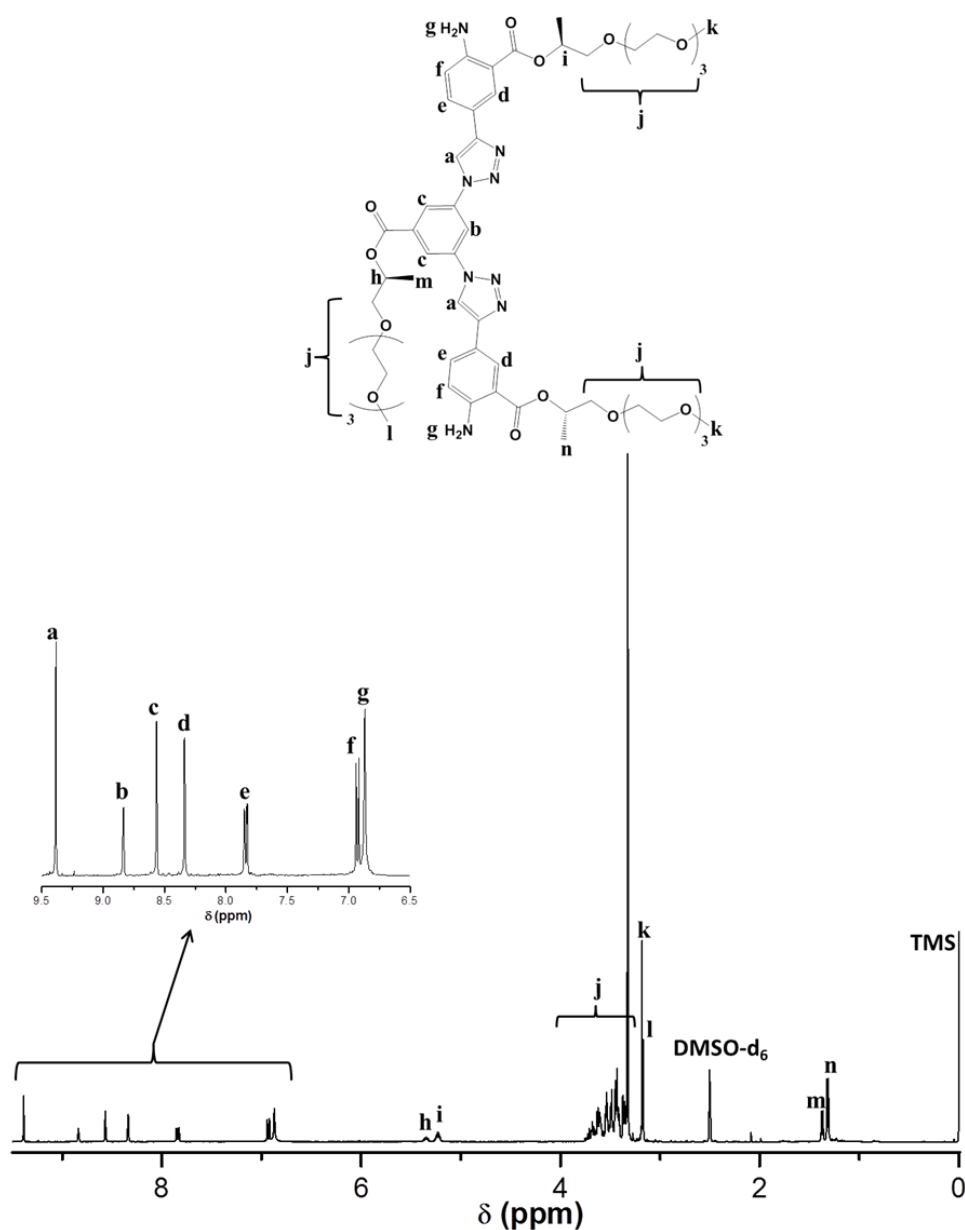


Figure 4.3. ^1H NMR spectrum of **30** in DMSO-d_6 .

Successful characterization of this amphiphilic molecule was followed by investigation of the self-assembly behavior. Self-assembly studies were carried out in $\text{H}_2\text{O}/$ acetonitrile and $\text{H}_2\text{O}/$ DMF solvent solutions. Transmission electron microscopy (TEM), UV-vis and CD spectrometry were used to confirm self-assembly. Results were obtained through direct experimentation varying solvent compositions, temperature and concentration. Figure 4.4 shows UV-vis spectra of solvent dependent and concentration dependent studies carried out on **30**.

4.2.2.3 Analysis of aggregation behavior

UV-vis

First we carried out a concentration dependent study with concentrations ranging from 0.0035 mM to 0.018 mM dissolved in a 90:10 H₂O/ DMF solution. All samples were completely solvated because of the increased solubility of **30**. Concentration dependent studies show an increase in absorption with increase in concentration. This did not effectively prove aggregation had taken place.

Subsequently a solvent dependent preliminary study was carried out to show the good/ bad solvent composition at which **30** shows signs of aggregation (Figure 4.4a). Solvent dependent studies were carried out in H₂O/ DMF solutions ranging from 10:90 H₂O/ DMF to 100:0 H₂O/ DMF. A decrease in absorption was observed when the H₂O content was increased. Absorption values at wavelength 279 nm were plotted against the H₂O content, indicating hypochromicity induced by aggregation (Figure 4.4b).

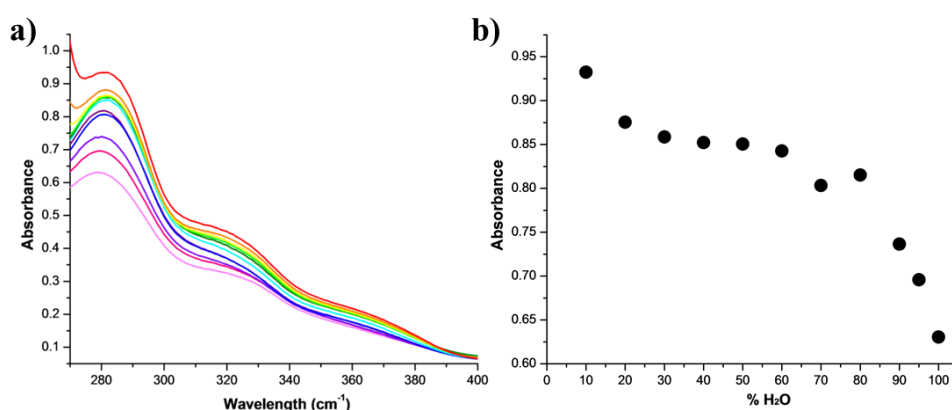


Figure 4.4. UV-vis spectra of **30** (a) Solvent dependent studies (red line = 10:90 H₂O/ DMF, lilac line = 100:0 H₂O/ DMF), (b) Absorbance at 279 nm plotted against the H₂O content.

Circular dichroism

Figure 4.5 shows a solvent dependent CD-spectrum of **30**. Observed Cotton effects confirmed helix formation. It is expected that the sample with the highest water content will give the greater Cotton effect, but in this case the higher the water content the smallest the intensity of the Cotton effect. A possible reason for this could be that the system is in a kinetic trap causing mismatches in the screw sense. The larger the water content, the less dynamic the system becomes. This may limit the CD intensity.

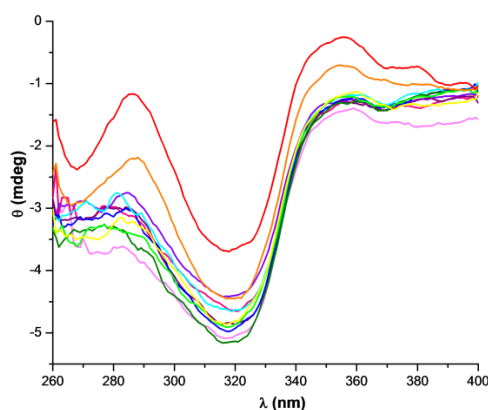


Figure 4.5. CD spectra of solvent dependent studies of **30** (red line = 100:0 H₂O/ DMF, lilac line = 10:90 H₂O/ DMF).

These findings were supported by TEM images of **30** carried out in a 100% H₂O solution (Figure 4.6). These images showed bundled, thread-like helical structures confirming UV-vis and CD results.

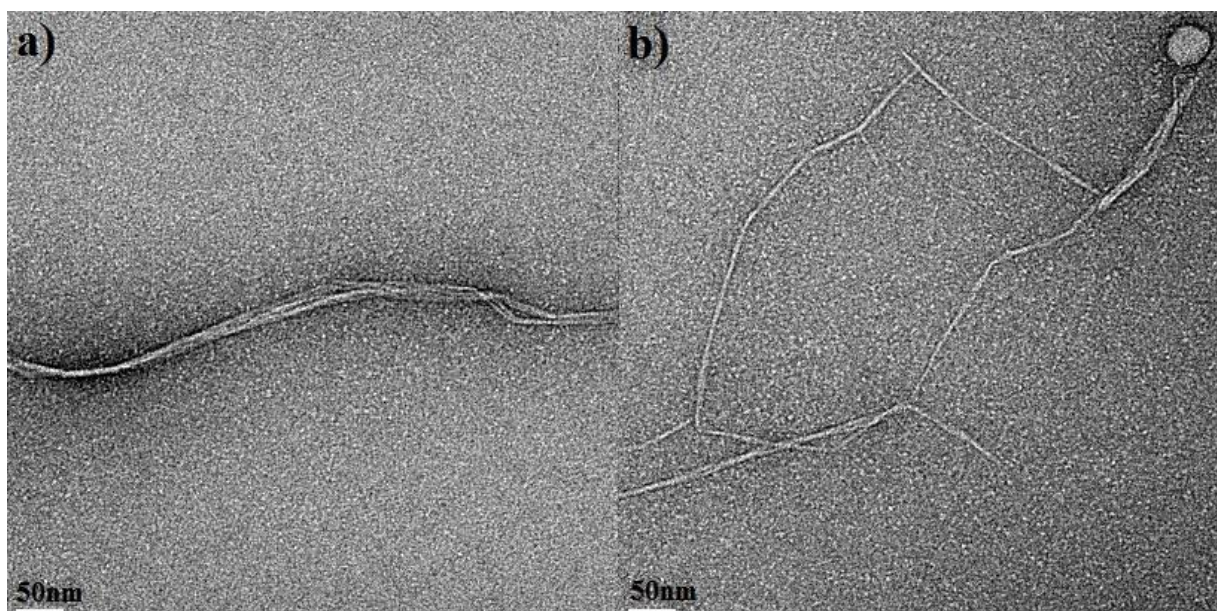


Figure 4.6. TEM images of **30** in H₂O.

4.3 Conclusions

Discotic amphiphiles bearing chiral polar side chains for self-assembly were successfully synthesized via the copper catalyzed click reaction. Self-assembly of these structures were investigated using UV-vis, CD spectroscopy, and TEM microscopy. UV-vis spectra confirmed aggregation of molecules and CD data showed evidence of helical formation. The formation of bundled helical aggregates was confirmed by TEM images.

4.4 Materials and Methods

4.4.1 Materials

General information is given in 3.4.

TEM analyses were done on a LEO912 TEM instrument operating with an accelerating voltage of 120 kV. UV-vis and CD titrations were prepared by varying the solvent composition and the concentration respectively. It was carried out in spectrophotometric grade acetonitrile and DMF and distilled water. UV-vis spectra were obtained using Specord® 210 Plus. CD measurements were made using a Chirascan Plus Spectropolarimeter. UV-vis and CD spectroscopy experiments were carried out at 25 °C, unless stated otherwise. Optical rotations were carried out on an ADP220 Automatic polarimeter.

4.4.2 Experimental Procedures

Synthesis of (S)-methyl 2-(((S)-tetrahydro-2H-pyran-2-yl)oxy)propanoate (17)

(S)-Methyl 2-hydroxypropanoate, **16**, (10 g, 96 mmol) and 3,4-dihydro-2H-pyran (13.2 g, 0.156 mole) was mixed and cooled to 0 °C before 3 drops of concentrated HCl was added. The reaction was stirred for 10 hours and reached room temperature on its own accord. Na₂CO₃ (3 g, 0.028 mmol) was added and it was allowed to stir for another 10 hours. After completion of the reaction it was filtered and concentrated to a smaller volume. Subsequently it was purified by distillation (69-76 °C, 29 mmHg).³³ (78% yield) **¹H NMR** (400 MHz, CDCl₃) δ ppm 1.44 – 1.36 (m, 3H), 1.89 – 1.46 (m, 6H), 3.53 – 3.39 (m, 1H), 3.71 (d, *J* = 1.4 Hz, 3H), 3.93 – 3.78 (m, 1H), 4.30 (dq, *J* = 87.1, 6.9 Hz, 1H), 4.67 (dt, *J* = 7.3, 3.6 Hz, 1H). **¹³C NMR** (101 MHz, CDCl₃) δ ppm 18.12, 18.92, 19.27, 19.31, 25.36, 25.47, 30.48, 30.57, 52.00, 52.02, 62.55, 62.57, 70.07, 72.49, 97.73, 98.41, 173.81, 173.92.

Synthesis of (S)-2-(((S)-tetrahydro-2H-pyran-2-yl)oxy)propan-1-ol (18)

A slurry of LiAlH₄ (3.75 g, 98.8 mmol) and dry Et₂O (50 mL) was cooled in an ice bath. **17** was dissolved in dry Et₂O (50 mL) and added dropwise to the LiAlH₄ slurry. The reaction was allowed to stir at 0 °C for 8 hours. Subsequently it was allowed to reach room temperature and stirred for another 12 hours before it was refluxed for 5 hours. The reaction was quenched by a dropwise addition of 80 mL ethyl acetate followed by 10% NaOH solution (10 mL) and water (40 mL). The crude product was purified by distillation (60-65 °C, 30 mmHg).³³⁻³⁵ (80% yield) **¹H NMR** (400 MHz, CDCl₃) δ ppm 1.18 (dd, *J* = 34.9, 6.5 Hz, 3H), 1.92 – 1.41 (m, 8H), 3.70 – 3.43 (m, 4H), 4.04 – 3.78 (m, 2H), 4.64 (ddd, *J* = 9.0, 5.5, 2.4 Hz, 1H). **¹³C NMR** (101 MHz,

CDCl₃) δ ppm 17.29, 17.81, 20.14, 21.00, 25.18, 25.44, 31.17, 31.67, 63.24, 64.64, 66.25, 67.27, 74.96, 77.75, 99.14, 99.99.

Synthesis of 2-((S)-2,5,8,11-tetraoxatetradecan-13-yloxy)tetrahydro-2H-pyran (19)

(S)-2-(((S)-tetrahydro-2H-pyran-2-yl)oxy)propan-1-ol, **18**, (3 g, 18.7 mmol), 2-(2-(2-methoxyethoxy)ethoxy)ethyl 4-methylbenzenesulfonate (6.72 g, 21 mmol), and sodium hydride (1.27 g, 52.9 mmol) was added to dry THF (100 mL) and refluxed for 12 hours. After completion of the reaction, water was added to quench the reaction. The THF was removed under reduced pressure and the water was extracted with dichloromethane and ethyl acetate (2 x 50 mL each). The organic phases were combined and the solvent was removed (70% yield). The product was taken to the next reaction without further purification as mentioned by reference.³⁶ **¹H NMR** (400 MHz, CDCl₃) δ ppm 0.87 (dt, J = 10.6, 6.8 Hz, 1H), 1.14 (t, J = 6.3 Hz, 2H), 1.26 (s, 3H), 1.95 – 1.41 (m, 6H), 3.38 (s, 3H), 3.76 – 3.40 (m, 14H), 4.02 – 3.91 (m, 1H).

Synthesis of (S)-2,5,8,11-tetraoxatetradecan-13-ol (20)

2-(((S)-2,5,8,11-tetraoxatetradecan-13-yloxy)tetrahydro-2H-pyran, **19**, (3.54 g, 11.6 mmol) was dissolved in methanol (50 mL) and cooled to 0 °C. *p*-Toluenesulfonic acid monohydrate (13.2 g, 69.6 mmol) was added at 0 °C and the reaction was allowed to stir for 4 hours while reaching room temperature on its own accord. A saturated sodium bicarbonate solution (50 mL) was added before it was extracted with ethyl acetate. The aqueous phase was saturated with salt and extracted with dichloromethane. The organic phases were combined and purified by column chromatography (5:1 ethyl acetate: acetone) and product was obtained in 41% yield. **¹H NMR** (400 MHz, CDCl₃) δ ppm 1.02 (d, J = 6.4 Hz, 3H), 2.86 (s, 1H), 3.18 (dd, J = 9.8, 8.2 Hz, 1H), 3.27 (s, 3H), 3.37 (dd, J = 9.8, 3.0 Hz, 1H), 3.57 – 3.43 (m, 12H), 3.86 (pd, J = 6.5, 3.0 Hz, 1H). **¹³C NMR** (101 MHz, CDCl₃) δ ppm 18.55, 59.06, 66.30, 70.51, 70.52, 70.60, 70.61, 71.97.

Synthesis of 3,5-diazidobenzoic acid (22)

3,5-Diaminobenzoic acid, **21**, was dissolved (1 g, 6.6 mmol) into THF (60 mL) and cooled to 0 °C. Subsequently *tert*-butyl nitrite (7.45 g, 0.072 mmol) in THF (5 mL) was added dropwise over 15 minutes at 0 °C. After stirring for 5 minutes, a mixture of trimethylsilyl azide (4.54 g, 0.039 mol) in THF (5 mL) was added dropwise over 10 minutes and allowed to stir at 0 °C for 30 minutes. Then it was allowed to stir at room temperature for another 30 minutes and followed by TLC. After completion of the reaction 5 spoons of silica gel and 5 spoons of MgSO₄ was added to the mixture and

it was allowed to stir for 2 hours before it was filtered to give the relatively pure desired product. $^1\text{H NMR}$ (400 MHz, DMSO- d_6) δ ppm 7.04 (t, $J = 2.1$ Hz, 1H), 7.38 (d, $J = 2.1$ Hz, 2H).

Synthesis of (S)-2,5,8,11-tetraoxatetradecan-13-yl 3,5-diazidobenzoate (23)

3,5-Diazidobenzoic acid, **22**, (0.15 g, 0.73 mmol) and (S)-2,5,8,11-Tetraoxatetradecan-13-ol, **20**, (0.195 g, 0.88 mmol) was dissolved in THF (20 mL) and cooled to 0 °C. *N,N'*-Dicyclohexylcarbodiimide (DCC) (0.18 g, 0.88 mmol) was added and after 2 minutes it was followed by the addition of 4-dimethylaminopyridine, DMAP, (0.011 g, 0.088 mmol). The mixture was stirred overnight reaching room temperature on its own accord. After completion of the reaction the THF was removed and water was added. The aqueous phase was extracted with ethyl acetate (4 x 50 mL) and the product purified by column chromatography (1:1 pentane: ethyl acetate) (32% yield). The crude product was taken to the next reaction without further purification in order to exclude any decomposition occurring.

Synthesis of (S)-2,5,8,11-tetraoxatetradecan-13-yl 3,5-bis(4-phenyl-1H-1,2,3-triazol-1-yl)benzoate (24)

(S)-2,5,8,11-Tetraoxatetradecan-13-yl 3,5-diazidobenzoate, **23**, (38.7 mg, 0.094 mmol) and phenylacetylene (48.4 mg, 0.47 mmol) was taken up into dimethylformamide (DMF) (1 mL). Copper(I) bromide (1.4 mg, 9.47 μ mol), pentamethyldiethylenetriamine (PMDETA) (4.9 mg, 0.028 mmol), and ascorbic acid (0.33 mg, 1.89 μ mol) was added to the reaction mixture and it was stirred overnight at room temperature. An aqueous workup was performed and the crude product was extracted with ethyl acetate and dichloromethane. The product was purified by column chromatography (1:1 pentane:ethyl acetate) (67% yield). $^1\text{H NMR}$ (300 MHz, CDCl_3) δ ppm 0.07 (s, 3H), 3.31 (s, 3H), 3.80 – 3.52 (m, 14H), 5.48 – 5.40 (m, 1H), 7.52 – 7.36 (m, 6H), 7.98 – 7.90 (m, 4H), 8.49 (s, 2H), 8.51 (d, $J = 2.1$ Hz, 2H), 8.65 (t, $J = 2.1$ Hz, 1H).

Synthesis of 2-azido-5-iodobenzoyl chloride (26)

2-Azido-5-iodobenzoic acid, **25**, (1.5 g, 0.0052 mmol) was dissolved in SOCl_2 (60 mL) and refluxed for 2½ hours. After completion of the reaction excess SOCl_2 was removed. The remaining residue (red solid) was dried on a vacuum pump overnight. The product was taken to the next reaction without purification. $^1\text{H NMR}$ (400 MHz, CDCl_3) δ ppm 7.03 (d, $J = 8.5$ Hz, 1H), 7.90 (dd, $J = 8.5, 2.1$ Hz, 1H), 8.37 (d, $J = 2.1$ Hz, 1H).

Synthesis of (S)-2,5,8,11-tetraoxatetradecan-13-yl 2-azido-5-iodobenzoate (27)

(S)-2,5,8,11-tetraoxatetradecan-13-ol, **20**, (1.27 g, 0.0057 mol), triethylamine (0.63 g, 6.27 mmol), and 4-dimethylaminopyridine (DMAP) (7.7 mg, 0.063 mmol) was mixed together and cooled to 0 °C. 2-Azido-5-iodobenzoyl chloride, **26**, was added at 0 °C and the reaction was stirred until completion. The crude product was purified by column chromatography (1:1 pentane:ethyl acetate) (59.6% yield). ¹H NMR (400 MHz, CDCl₃) δ ppm 1.33 (d, *J* = 6.5 Hz, 3H), 3.35 (s, 3H), 3.71 – 3.48 (m, 14H), 5.28 (pd, *J* = 6.4, 4.3 Hz, 1H), 6.95 (d, *J* = 8.5 Hz, 1H), 7.76 (dd, *J* = 8.5, 2.1 Hz, 1H), 8.08 (d, *J* = 2.1 Hz, 1H). ¹³C NMR (101 MHz, CDCl₃) δ ppm 16.73, 59.09, 70.58, 70.69, 70.72, 70.83, 70.98, 72.00, 73.58, 87.44, 121.79, 124.93, 140.00, 140.25, 141.72, 163.33.

Synthesis of (S)-2,5,8,11-tetraoxatetradecan-13-yl 2-amino-5-((trimethylsilyl)ethynyl)benzoate (28)

(S)-2,5,8,11-tetraoxatetradecan-13-yl 2-azido-5-iodobenzoate, **27**, (0.44 g, 0.89 mmol) and ethynyltrimethylsilane (0.114 g, 1.1 mmol) was taken up in a 1:1 THF/TEA solution (5 mL). The solution was degassed with one freeze-pump-thaw cycle before Pd(PPh₃)₄ (20.6 mg, 0.017 mmol), and copper(I) iodide (3.39 mg, 0.017 mmol) was added. Subsequently three more freeze-pump-thaw cycles was carried out to degass the system. The reaction was run at 30 °C for two days. TLC indicated that the azide groups were not completely reduced to amine groups. Reaction mixture was filtered and 5 spoons of silica gel and ethyl acetate (100 mL) was added. It was stirred for 1 hour before it was filtered and the solvent removed. To reduce all of the azide groups to amines, the crude product was taken up into a 9:1 THF:water mixture (20 mL) together with triphenylphosphine (1.17 g, 4.48 mmol) and stirred at 30 °C for 3 hours. TLC indicated completion of the reaction. Crude product was taken to the next reaction without further purification.

Synthesis of (S)-2,5,8,11-tetraoxatetradecan-13-yl 2-azido-5-ethynylbenzoate (29)

Crude (S)-2,5,8,11-tetraoxatetradecan-13-yl-2-amino-5-((trimethylsilyl)ethynyl)benzoate, **28**, and tetra-*n*-butylammonium fluoride (TBAF) (1.17 g, 4.4 mmol) was dissolved in 10 mL dichloromethane and stirred for 5 minutes. After completion the solvent was removed and the crude product was purified by column chromatography (1:1 pentane: ethyl acetate). A second purification by column chromatography was done to get rid of the excess triphenylphosphine (2:1 ethyl acetate: pentane) (66.7% yield). ¹H NMR (300 MHz, CDCl₃) δ ppm 1.33 (t, *J* = 6.9 Hz, 3H), 3.37 (s, 3H), 3.75 –

3.51 (m, 14H), 5.28 (pd, $J = 6.4, 4.4$ Hz, 1H), 5.96 (s, 2H), 6.59 (d, $J = 8.5$ Hz, 1H), 7.34 (dd, $J = 8.5, 2.0$ Hz, 1H), 8.02 (d, $J = 2.0$ Hz, 1H).

Di((S)-2,5,8,11-tetraoxatetradecan-13-yl) 5,5'-(1,1'-(5-((S)-3-methyl-2,5,8,11,14-pentaoxapentadecan-1-oyl)-1,3-phenylene)bis(1H-1,2,3-triazole-4,1-diyl))bis(2-aminobenzoate) (30)

(S)-2,5,8,11-tetraoxatetradecan-13-yl 3,5-diazidobenzoate, **23**, (78.3 mg, 0.192 mmol), (S)-2,5,8,11-tetraoxatetradecan-13-yl 2-azido-5-ethynylbenzoate, **29**, (0.175 g, 0.479 mmol), copper(I) bromide (2.7 mg, 0.019 mmol), pentamethyldiethylenetriamine (PMDETA) (9.96 mg, 0.057 mmol), and ascorbic acid (0.675 mg, 3.83 μ mol) was taken up in DMF (2 mL). The reaction was stirred at room temperature for 30 hours. Subsequently the solvent was evaporated and the product was purified by column chromatography (ethyl acetate + 10% methanol) (64% yield). **¹H NMR** (400 MHz, DMSO- d_6) δ ppm 1.32 (d, $J = 6.4$ Hz, 6H), 1.37 (d, $J = 6.5$ Hz, 3H), 3.17 (s, 3H), 3.18 (s, 6H), 3.44 – 3.30 (m, 42H), 5.23 (td, $J = 6.5, 4.1$ Hz, 2H), 5.35 (td, $J = 6.6, 3.9$ Hz, 1H), 6.87 (s, 4H), 6.93 (d, $J = 8.7$ Hz, 2H), 7.84 (dd, $J = 8.6, 2.1$ Hz, 2H), 8.34 (d, $J = 2.2$ Hz, 2H), 8.57 (d, $J = 2.0$ Hz, 2H), 8.84 (t, $J = 2.0$ Hz, 1H), 9.39 (s, 2H). **¹³C NMR** (101 MHz, DMSO- d_6) δ ppm 0.00, 16.27, 16.53, 57.85, 57.86, 69.28, 69.40, 69.59, 69.62, 69.70, 69.99, 71.08, 71.09, 71.26, 72.50, 72.68, 109.14, 115.09, 116.51, 117.14, 118.17, 119.21, 127.54, 131.38, 133.22, 137.89, 147.61, 151.27, 163.46, 166.63.

4.5 References

- (1) Block, M. A. B. *Folding Architectures Containing Phenylene Ethynylene Oligomers and Polymers*, 2006.
- (2) Yu, S. M.; Lib, Y.; Kim, D. *Soft Matter* **2011**, *7*, 7927.
- (3) Katsaras, J.; Prosser, R. S.; Stinson, R. H.; Davis, J. H. *Biophys. J.* **1992**, *61*, 827.
- (4) Kelkar, D. A.; Chattopadhyay, A. *Biochim. Biophys. Acta* **2007**, *1768*, 2011.
- (5) Watson, J. D.; Crick, F. H. C. *Nature* **1953**, *171*, 737.
- (6) Ishihara, S.; Furuki, Y.; Takeoka, S. *Polym. Adv. Technol.* **2008**, *19*, 1097.
- (7) Banno, M.; Yamaguchi, T.; Nagai, K.; Kaiser, C.; Hecht, S.; Yashima, E. *J. Am. Chem. Soc.* **2012**, *134*, 8718–8728.
- (8) Ray, C. R.; S. Moore, J. *Adv. Polym. Sci.* **2005**, *177*, 91.
- (9) Hill, D. J.; Mio, M. J.; Prince, R. B.; Hughes, T. S.; Moore, J. S. *Chem. Rev. (Washington, DC, U. S.)* **2001**, *101*, 3893.
- (10) Nakano, T.; Okamoto, Y. *Chem. Rev. (Washington, DC, U. S.)* **2001**, *101*, 4013.
- (11) Cornelissen, J. J. L. M.; Rowan, A. E.; Nolte, R. J. M.; Sommerdijk, N. A. J. M. *Chem. Rev. (Washington, DC, U. S.)* **2001**, *101*, 4039.
- (12) Shetty, A. S.; Zhang, J.; Moore, J. S. *J. Am. Chem. Soc.* **1996**, *118*, 1019.
- (13) Brunsveld, L.; Folmer, B. J. B.; Meijer, E. W.; Sijbesma, R. P. *Chem. Rev. (Washington, DC, U. S.)* **2001**, *101*, 4071.
- (14) Juricek, M.; Felici, M.; Contreras-Carballada, P.; Lauko, J.; Bou, S. R.; Kouwer, P. H. J.; Brouwerb, A. M.; Rowan, A. E. *J. Mater. Chem.* **2011**, *21*, 2104.
- (15) Tanaka, M.; Ikeda, T.; Mack, J.; Kobayashi, N.; Haino, T. *J. Org. Chem.* **2011**, *76*, 5082.
- (16) Besenius, P.; Portale, G.; Bomans, P. H. H.; Janssen, H. M.; Palmans, A. R. A.; Meijer, E. W. *Proc. Natl. Acad. Sci. USA* **2010**, *107*, 17888.
- (17) Tornøe, C. W.; Christensen, C.; Meldal, M. *J. Org. Chem.* **2002**, *67*, 3057.
- (18) Juricek, M.; Kouwer, P. H. J.; Rowan, A. E. *Chem. Commun. (Cambridge, U. K.)* **2011**, *47*, 8740.
- (19) Schweinfurth, D.; Hardcastleb, K. I.; Bunz, U. H. F. *Chem. Commun. (Cambridge, U. K.)* **2008**, 220.
- (20) Steenis, D. J. V. C. v.; David, O. R. P.; Strijdonck, G. P. F. v.; Maarseveen, J. H. v.; Reek, J. N. H. *Chem. Commun. (Cambridge, U. K.)* **2005**, 4333.
- (21) Wyszogrodzka, M.; Haag, R. *Chem. Eur. J.* **2008**, *14*, 9202.
- (22) Ornelas, C.; Aranzaes, J. R.; Cloutet, E.; Alves, S.; Astruc, D. *Angew. Chem., Int. Ed.* **2007**, *46*, 872
- (23) Lahiri, S.; Thompson, J. L.; Moore, J. S. *J. Am. Chem. Soc.* **2000**, *122*, 11315.
- (24) Zhao, D.; Moore, J. S. *Chem. Commun. (Cambridge, U. K.)* **2003**, 807.
- (25) Kubel, C.; Mio, M. J.; Moore, J. S.; Martin, D. C. *J. Am. Chem. Soc.* **2002**, *124*, 8605.
- (26) Greef, T. F. A. D.; Smulders, M. M. J.; Wolffs, M.; Schenning, A. P. H. J.; Sijbesma, R. P.; Meijer, E. W. *Chem. Rev. (Washington, DC, U. S.)* **2009**, *109*, 5687.
- (27) Cantekin, S.; Eikelder, H. M. M. t.; Markvoort, A. J.; Veld, M. A. J.; Korevaar, P. A.; Green, M. M.; Palmans, A. R. A.; Meijer, E. W. *Angew. Chem., Int. Ed.* **2012**, *51*, 6426.
- (28) Cat, I. D.; Guo, Z.; George, S. J.; Meijer, E. W.; Schenning, A. P. H. J.; Feyter, S. D. *J. Am. Chem. Soc.* **2012**, *134*, 3171.
- (29) Pfukwa, R.; Kouwer, P. H. J.; Rowan, A. E.; Klumperman, B. *manuscript in preparation* **2012**.
- (30) Brunsveld, L.; Zhang, H.; Glasbeek, M.; Vekemans, J. A. J. M.; Meijer, E. W. *J. Am. Chem. Soc.* **2000**, *122*, 6175.

- (31) Herrikhuyzen, J. v.; Syamakumari, A.; Schenning, A. P. H. J.; Meijer, E. W. *J. Am. Chem. Soc.* **2004**, *126*, 10021.
- (32) Palmans, A. R. A.; Vekemans, J. A. J. M.; Havinga, E. E.; Meijer, E. W. *Angew. Chem., Int. Ed. Engl.* **1997**, *36*, 2648.
- (33) Chiellini, E.; Galli, G.; Carrozzino, S.; Gallot, B. *Macromolecules* **1990**, *23*, 2106.
- (34) Ghirardelli, R. G. *J. Am. Chem. Soc.* **1973**, *95*, 4987.
- (35) Perkins, M. V.; Kitching, W.; Konig, W. A.; Drew, R. A. I. *J. Chem. Soc., Perkin Trans. 1* **1990**, 2501.
- (36) Hirose, T.; Matsuda, K.; Irie, M. *J. Org. Chem.* **2006**, *71*, 7499.

Chapter 5 Conclusions

Dendrimers are well-defined, “tree-like” macromolecules, with a high degree of order, due to their well-defined spatial location of functional groups, contributing to their specific function.^{1,2} π -Conjugated dendrimers are particularly interesting to us because of their potential applications in light harvesting, fluorescent sensors, light emitting diodes and devices based on nonlinear optical interactions.³

Firstly the packing of a conjugated phenyl isoxazole dendritic system was investigated. It was anticipated that the alternating phenyl isoxazole system will have a flat packing arrangement, but steric hindrance at higher generations would cause this dendrimer system to deviate from the flat packing arrangement to adopt a fan-like out-of-plane structure.

Successful synthesis of the isoxazole linker moiety was achieved in a model reaction by using sodium hypochlorite to couple an oxime and a terminal alkyne. Convergent and divergent pathways were attempted to synthesize the phenyl isoxazole dendrimers, but synthesis of the second and third generation was not successful.

Scientists are constantly trying to simplify the tedious and repetitive nature of chemical syntheses as much as possible. A vast amount of research has gone into the development of systems in which low molar mass compounds autonomously assemble to produce large, ordered, aggregates.

Discotic amphiphilic molecules are known to self-assemble into helical or columnar aggregates. We investigated the ability of discotic amphiphilic molecules based on a conjugated phenyl triazole discotic core tethered with chiral polar side chains to self-assemble into helical supramolecules. These discotic amphiphiles were successfully synthesized via the copper-catalysed click reaction. Self-assembly of these structures was investigated using UV-vis, CD spectroscopy, and TEM microscopy. UV-vis spectra confirmed aggregation of molecules and CD data showed evidence of helix formation. The formation of bundled helical aggregates was confirmed by TEM images

Future work

It was speculated that the chirality of the discotic amphiphiles was the driving force behind the self-assembly. It would be interesting to develop and investigate similar

amphiphilic materials minus the chiral centres. The functionality of chiral information will become evident when the chiral and achiral molecules' self-assembly is compared to each other.

Fluorescent tag-based methodology is a promising candidate for characterization of self-assembly. A fluorescent tag can be attached to one side chain of the amphiphilic discotic molecules to visualize their self-assembly process with confocal fluorescence microscopy in real time.⁴ This will effectively provide evidence of helical or columnar stacking as well as the rate of the self-assembly.

References

- (1) Balzani, V.; Ceroni, P.; Maestri, M.; Vicinelli, V. *Current Opinion in Chemical Biology* **2003**, 657.
- (2) Carlmark, A.; Hawker, C.; Hulta, A.; Malkoch, M. *Chem. Soc. Rev.* **2009**, 38, 352.
- (3) Melinger, J. S.; Davis, B. L.; McMorrow, D.; Pan, Y.; Peng, Z. *J. Fluoresc.* **2004**, 14, 105.
- (4) Ruan, J.; Raghunathan, S.; Hartley, J. G.; Singh, K. V.; Akin, H. E.; Portney, N. G.; Ozkan, M. *American Institute of Physics Conference Proceedings* **2007**, 931, 462.